OSTI Test Form; April 24, 1962

NATIONAL AERONAUTICS AND SPACE ADMINISTRATION
Office of Scientific and Technical Information

Document Transmittal Form (NASA TM X-51207)

This transmittal form is intended to guide the Office of Scientific and Technical Information in processing scientific and technical reports and articles prepared under NASA contracts, subcontracts, and grants. It is also a processing guide for reports and articles produced by NASA activities when these publications do not appear in the regular NASA reports series (e.g., Technical Report, Technical Note, Technical Memorandum, Technical Translation, etc.).

The form is to accompany each unclassified and classified document transmitted for central indexing and reference or for processing and distribution. One copy of this form, accompanied by one or more copies of the document, should be sent to the following address:

X64 10581 *

National Aeronautics and Space Administration
Office of Scientific and Technical Information
Code AFSD-O
Washington 25, D. C.

CODE 2A

One of the types listed on the reverse side of this form (indicated by a numeral, and modified where necessary by alphabetical subheadings) should be selected for each document submitted. The following identifying information should also be furnished:

Document Title: A Summary Review of the Scientific Findings of the Mariner Venus Mission

Originating Organization: Ames Report No. _____

Date of Document: _____ No. of Copies Enclosed: _____

Security Classification of Document: _____
If classified: Title Classification: _____ Abstract Classification: _____

Contract, Sub-Contract, or Grant No. _____

NASA Office Transmitting Document: _____

By: _____
(Signature and Title)

Date Transmitted: _____

Document Type: _____ (Appropriate numeral and letter selected from back.)

Document Types

1. ____ Report is unclassified and is suitable for unlimited announcement and distribution to the aeronautics and space community, and for public sale.

2. ____ Report is unclassified, but contains information of limited usefulness and does not justify widespread automatic distribution to the aeronautical and space community. It can, however, be announced and made publicly available.

3. V Report is unclassified, but for official reasons, must be restricted as follows:

   a. ____ Government agencies and their contractors only.
   b. ____ Government agencies only.
   c. X NASA activities only.

4. ____ Report bears a security classification and is suitable for distribution within the limits of security considerations to:

   a. ____ Government agencies and their contractors only.
   b. ____ Government agencies only.
   c. ____ NASA activities only.

5. ____ Reprint of a journal article reporting NASA-supported work.

6. ____ Article prepared for journal publication (preprint or other copy) reporting NASA-supported work. (Normally handled as No. 2 above.)

   Estimated date of publication:_____

7. ____ Material for presentation at a meeting or conference
   Name of Meeting:_____ Date:_____
   Sponsor(s):_____

   a. ____ Scheduled for publication in proceedings. (Normally handled as No. 2 above.)

      Estimated date of publication:_____

   Not scheduled for publication in proceedings and subject to the following limitations or announcement and dissemination:

   b. ____ Government agencies and their contractors only.
   c. ____ Government agencies only.
   d. ____ NASA activities only.

N65-88983
~~N64 10581~~ *

A SUMMARY REVIEW OF THE SCIENTIFIC FINDINGS OF THE MARINER VENUS MISSION**

Charles P. Sonett

Space Sciences Division
NASA. Ames Research Center
Moffett Field, Calif.

CODE 2
proof copy
[1963] 62p refs
[6] conf
(NASA TM X-51207)
10581

ABSTRACT

A summary review of the scientific findings of Mariner II is given insofar as available data allow. The instruments and those characteristics of the total rocket system which affect the scientific experiments are described. The review covers both planetary and interplanetary results and provides descriptive material on the instruments. uncl.
Author

A. INTRODUCTION

Between 1959 and 1962 the United States launched three spacecraft, Pioneer IV, Pioneer V, and Mariner II, which spent an important amount of time in deep interplanetary space free of influences such as the Earth and the Moon. Mariner II also executed a hyperbolic near-collision course with the planet Venus during which time several scientific observations of the planet were made. In total, three kinds of observations can be technically abstracted from the Mariner II mission: interplanetary, planetary encounter, and those from the surface of the

---

*Portions of this paper were presented at the ~~One-hundredth~~ 100th Annual Meeting of the ~~National~~ Academy of Sciences, Washington, ~~D. C.,~~ ~~April~~ (22-24) 1963. Submitted for Publication

+To appear in Space Science Reviews, vol. 2, no. 6.

Available to NASA Offices and NASA Centers Only.

Earth. This discussion shall be limited to the particles and fields measurements and to the encounter measurements of Mariner II and shall not attempt to include in detail those experiments conducted from the surface of the Earth, in which the spacecraft was used as a radio probe. Those measurements made directly from the ground using optical techniques[1] or radar measurements[2] will not be discussed. The importance of these Earth-bound measurements must not be underestimated, for they are critical to a better understanding of the planet.

Mariner II (fig. 1) was launched on August 27, 1962 into a minimum energy orbit designed to intersect the orbit of Venus some three months later. The total mission consisted of two firings separated by several weeks - the time required to clear the launch pad and to erect and check out the second rocket.

Because of the paucity of published results on Mariner at the time of closing this paper, it is not possible to make anything like a critical review.[3] Therefore the intent is essentially descriptive, though the gross aspects of the various scientific findings as they are presently known are discussed. Both from the standpoint of available information and the breadth of the many disciplines involved, any attempt at scholastic completeness of each subject would be a task of Augean proportions. Thus the reader is urged, for example, in the case of the Venus atmosphere experiments and the interplanetary plasma and field

Available to NASA Offices and
NASA Centers Only.

experiments, to consider the array of available literature as the proper background. This material, largely being left out, is nevertheless to be considered as the appropriate framework within which each result should be critically discussed.

Since the instrumentation aboard Mariner had a strong interdisciplinary flavor, discussion of the retrieved information suggests a subdivision into two distinct classes - interplanetary and Venusian, although as we shall see even this is in some sense artificial. We begin with a brief outline of the basic character of the spacecraft (fig. 2) forming as it does the very special kind of platform from which all measurements had to be made. The bus, or basic frame, consisted of a hexagon with a superstructure and an array of solar cells divided between two panels. During most of the flight, orientation was maintained fixed in a heliocentric system. The roll axis of the spacecraft, defined as the normal to the plane of the hexagon, was pointed toward the Sun. Control of the roll axis direction as well as the yaw and pitch axes was done by gas jets and by both Sun and Earth seekers.

B. SPACECRAFT ORIENTATION AND INJECTION INTO INTERPLANETARY ORBIT

Figure 3 shows the solar orbit of both Pioneer V and Mariner II, the two spacecraft which transmitted interplanetary data over a period of several months. Both orbits are similar from an interplanetary standpoint, covering a region extending from 0.7 to 1 astronomical unit

distant from the Sun. It is, moreover, a common characteristic of minimum energy trajectories made in the direction of Venus that the initial velocity vector of the spacecraft with respect to Earth is constrained to the backward hemisphere from the Earth's orbital velocity vector. Thus, the spacecraft spends the better part of a month or two in the immediate vicinity of the Earth, after which it rapidly departs inward to intersect the orbit of Venus.

The Mariner was injected into orbit by an Atlas D series booster followed by the Agena B stage ~~with~~ having a dual start capability. The second start of the Agena follows a coast period in near-Earth orbit to a point where minimum energy injection into an interplanetary transfer ellipse to Venus can be made. Technically the process consists of two injections, the first being into a near-Earth satellite orbit. Constraints upon the launch sequence include proper coverage for telemetry and command from island, ocean, and land stations at critical times as well as range safety firing lane requirements. Those familiar with this procedure can appreciate the complexity of even this portion of the launch sequence.

The process is diagrammed in Figure 4 showing the various steps. The time following step 9 and preceding step 10 is especially relevant to the magnetometer experiment since it is during the period of solar acquisition but prior to Earth acquisition that the spacecraft executes a free roll about the solar direction allowing an in-flight check of the prelaunch calibration procedure. It is in the time

period following step 10 that the velocity and position vectors of the spacecraft are accurately determined. From this information is developed the firing or midcourse maneuver program where a vector velocity increment is added so that precise intersection with Venus can take place. During this period a new orientation is established since the nozzle of the midcourse motor is fixed in the spacecraft and the addition of a velocity increment demands a specific orientation. During this period scientific data are not transmitted and solar power is not demanded. The steps in this process are illustrated in Figure 5.

The Experiments as a System

It is of general interest to summarize the instruments and experiments of Mariner.[4] The division of weight and power is shown in table I and table II lists the types of measurements. A data conditioning system, basically an encoder buffer, converts analog measurements into digital format and generally provides the sequence, or data train, for modulation of the transmitter. Data storage or buffering was provided for some of the cosmic ray experiments.

Specifically, two modes of operation were provided: cruise, for interplanetary space, and encounter when near Venus. The data cycle is represented by a "frame" consisting of 21 eight-bit words. Alternate transmission of this frame and the engineering data frame was

made during cruise, the latter being suppressed during encounter. The frame repetition rate was every 37 seconds during cruise corresponding to 8.33 bits/sec and being increased to once every 20 seconds during encounter. ~~Transmission of data is, of course, sequential.~~

C. ENCOUNTER

We shall consider first the encounter of Mariner with Venus and follow this with a discussion of the interplanetary ~~position~~ portion of the flight. The encounter geometry is illustrated in Figure 6. From the viewpoint of Venus, the spacecraft approached from above and behind the planet - that is, an overtaking collision began from above the plane of the planet's equator on the dark side and ended on the day side in the southern hemisphere. In a sense, all the instruments were party to the planetary measurements.

1. Microwave Emission

Microwave emission from Venus was first observed by Mayer, et al., at 3.15 cm where the intensity was twice that expected from a black body having an infrared temperature of Venus (225° K). The equivalent temperature continues to rise with wavelength until 3 cm, when it is about 600° K, until 21 cm.

Variations of disk temperature with solar phase are especially difficult to measure because of the great variation in distance between

conjunctions of the planet. Data regarding phase-temperature variation has been especially conflicting. Close planetary scanning thus can potentially yield information on both symmetric and asymmetric limb-limb brightness variations of value in separating emission and absorption models for the source of the "nonthermal" emission.

The wavelengths chosen for the microwave radiometer were based upon the following rationale. The investigations from Earth of the steady planetary radiation at wavelengths from 4 mm to 21 cm suggest a nonthermal emission because the flux increases anomalously toward longer wavelength. Contending hypotheses regarding the source include a hot surface with preferential atmospheric absorption, a strongly radiating ionosphere, atmospheric electricity, and dust friction (aeolosphere). Distinctions between these models are difficult to make because phase effects seem to be incapable of clean interpretation. Some models, notably the hot surface, favor limb darkening whereas the ionosphere model, as postulated, suggests limb brightening. Also solar insolation should be important only for certain models. In summary, a one-wavelength limb-limb scan would be expected to differentiate between an optically nondense ionosphere (limb-brightening) and a hot surface with selective atmospheric absorption (limb-darkening). In the latter instance, it is also necessary to make appropriate assumptions regarding the angular emission law for the surface (e.g., Lambertian). The choice of $\lambda = 19$ mm was made for this test, the exact wavelength

being partially dependent upon the availability of equipment from the Mariner A program. The 13.5-mm channel also included in this experiment resides at the center of a rotational band of H_2O. Then it follows that nonproportional limb absorption between the two channels should be indicative of the presence of H_2O.

In-flight calibrations of the microwave radiometer during the interplanetary cruise mode were made about every 4 days. A noise tube, as conventionally used in Earth-based calibration routines, was employed. Both gain and zero level shifts occurred in this equipment during cruise. The decrease in gain was the basis for the scan mode's not shifting into the slow (0.1°/sec) mode upon intercepting the planetary disk.

The scanning program was determined by the signal level of the microwave radiometer, and the performance of both this instrument and the IR detector had scans locked to the former. With a ~~gird~~ grid system defined by the ecliptic, the scan program is as depicted in Figure 7. Microwave radiometer amplifier in-flight changes are taken to be the cause of scan modifications which resulted in a modified data program. During the scan, the planetary distance necessarily varied. Thus the surface resolution was nonconstant.

The microwave instrument was a simplified design based upon a four-channel device originally intended for Mariner A. A Dicke switching system with alternate signal and free-space reference was

fed into a crystal video detector followed by an amplifier, synchronous detector, and filter with $\tau \simeq 20$ sec. The antenna system included an ~50-cm parabolic reflector with a serrated surface to eliminate specular reflection at optical wavelengths. Antenna beam widths were 2.2° and 2.5° with side lobe power down 23 db. A summary of the radiometer characteristics, taken from Barath, et al., is given in table III.

At the time of this writing only a preliminary reduction of the microwave radiometer data has been published.[5] This is restricted to the 19-mm channel. From the fortuitous circumstance of cancelling malfunctions in the scan mechanism a third scan was made across the sunlit hemisphere. The three scans yield

Dark side	460° ±69° K
Terminator	570° ±85° K
Light side	400° ±60° K

at 19 mm according to the experimenters. Thus, no significant difference in temperature occurs across the planet, implying either a surface heated uniformly or a hot atmosphere thoroughly mixed. In view of the clearly apparent limb darkening, the former choice is indicated. The indications from these data shown in Figure 8 are inconsistent with the ionosphere model, a view in keeping with the difficulty in maintaining sufficient ionosphere in the presence of

what appears to be an inadequate magnetic field, that is, insufficient magnetic inhibition of recombination.

Since these data have not been corrected for antenna beam width or for the time constant of the circuitry, the apparent limb darkening should be reduced to about half the value shown. The possibility of an ionosphere as the primary contributor to the centimeter brightness of the planet seems to be ruled out because the kind of ionosphere needed would just be approaching optical depth at 1 cm, in turn implying a limb brightening. Further, the lack of noticeable asymmetry in the first and last scans in Figure 8 is indicative of little dependence of the centimeter temperature upon the phase. In short, the observed limb darkening is consistent with the model of the Venusian environment having a high temperature originating deep in the atmosphere or at the surface of the planet.

The lack of a significant phase effect in the centimeter radiation from the planet suggests that the emitting layer is being heated in a manner relatively independent of the direction of the incident solar radiation. Since it appears unlikely that the planetary surface is being heated from below to the temperatures indicated, an attractive possibility is that strong lateral convective mixing must take place in the lower atmosphere of Venus. The primary heat source for the atmospheric engine would be the Sun with the heat being distributed in a uniform manner to the dark side. This possibility does not rule

out an aeolosphere model. On the other hand, any kind of a greenhouse model might be expected to display some kind of convective pattern; that is to say, a heat engine would exist with water perhaps playing a role in the creation of clouds and the establishment of a super-adiabatic lapse rate. However, even this kind of vertical convection does not satisfy the need for the lateral convection applied by the lack of a phase effect.

2. Infrared Profile

The problem of convective instability in the Venus atmosphere is suggested by the changeable cloud pattern seen by telescope from the Earth. At the time the experiments were designed for Mariner II, the question of convective instability of a cloudy layer seemed to be a problem of substance which could be attacked by means of a close scan of the planetary surface at appropriate wavelengths. The exact manner of this determination utilized a two-channel photometer with response centered at 10.4μ in a rotation-vibration band of CO_2 and at 8.4μ thought to be representative of a very transparent spectral region of the Venus atmosphere.

Thus the dual scan would be expected to display different brightness temperatures in the two channels if a mixture of carbon dioxide and other gases were being examined. Scanning of a cloud for which the scattering function is relatively independent of wavelength in

this interval should provide the same brightness temperature in both channels. A third alternative especially in situations where a strong vertical convection pattern exists might be a display of alternate regions corresponding to clouds and openings. Clearly, limb attenuation and phase effects might well be a product of such an experiment, especially with the relatively unknown makeup of the atmosphere.

The design of the instrument finally chosen is shown schematically in Figure 9 as taken from the papers of Chase, et al.[6,7] Reference to a disk whose temperature was measured directly was made at the end of the scan. The chopper made the detection synchronous; both channels swept together and were boresighted together with the microwave radiometer. The system employs conventional signal chopping and synchronous detection. Further details are to be found in the referenced literature.[7]

In Figure 10 are depicted the response curves for both IR channels. We have also reproduced from the paper of Chase, Kaplan, and Neugebauer the angular response of the 8μ channel (fig. 11). Reference for the demodulation was provided by a telescope observing free space. A "black-body" plate with a temperature-sensitive resistor provided a calibration check at the limit stop of each scan when the plate covered the viewing field of the photometer.

The substance of this experiment is contained in Figure 12 which shows the uncalibrated infrared radiometer data plotted against time. The scan pattern is the same as employed for the centimeter wave

radiometer. The three scans across the planet beginning with the dark side scan shown on the left of the figure followed by the terminator scan and the sunlit scan are displayed. The calibration sequences are interlaced as shown, both for the 8.9- and 10.4-micron channels. The calibration takes place at one end of the angular motion of the radiometers. Thus there is a double calibration in each instance. The slight difference in the levels for the two calibrations in a group is due to interference with structural members of the spacecraft for one case.

The experimenters report a slight limb darkening effect for the 10.4-micron channel. The figure shows a slight difference between the center and the limb scans. The difference being symmetric indicates that the temperatures measured are independent of the direction of solar lighting. The 8.9-micron data on the figure also show a limb darkening effect which is more pronounced than for the 10.4-micron channel and, furthermore, is asymmetric. This material cannot be discussed in an absolute context because of the lack of information regarding the calibration of the instrument and because of some difficulties with the circuitry. Nevertheless, the experimenters attribute of 10.4-micron channel data to a real effect which seems to indicate that extrapolation of these considerations to the 8-micron channel is real. It is to be noted that again a phase effect is lacking in the 10.4-micron channel as it was for the centimeter wave radiometers.

On the other hand, a slight phase effect seems to exist in the 8-micron channel. The most basic conclusions which can be drawn from this experiment are that both infrared radiometers look through essentially the same amount of atmosphere, and little if any irregularity was seen during the scan periods, indicating that if a cloud-top structure were being scanned, no breaks in the clouds were seen. It is concluded by the experimenters that a continuous cloudy region was being observed and that the transmittance of the medium between the radiometer and the scanned region was essentially the same for the two channels. A small amount of carbon dioxide seemed to be present in the upper atmosphere because of the slight limb darkening in the 10.4-micron channel. The stronger limb-darkening effect and its asymmetry in the 8-micron channel remains to be explained, but is presumably due to a stronger absorption effect and is ~~lightly~~ slightly dependent upon the direction of the incident solar radiation. The origin of the absorption remains open for speculation. It seems clear that the unbroken pattern in the data indicates that the clouds exist above a region of convective instability, that is to say, in a region in which an adiabatic or sub-adiabatic lapse rate exists. Therefore, this region may well not be connected with the lower regions of the atmosphere in the sense of a highly stirred medium. The slightly different temperatures seen in the two channels as compared to the differences seen in the calibrations further indicate a minor difference in brightness temperature, with the

carbon dioxide or 10.4-micron channel showing a slightly higher temperature than the 8-micron channel. Perhaps the most important conclusions to be drawn are the lack of an apparent pattern of convective instability together with a lack of a prominent phase effect, indicating, perhaps, that if a greenhouse effect exists, heat must be transported in an efficient manner from the sunlit hemisphere to the dark side and without an obvious pattern of convection at the altitudes of the uppermost clouds. An aeolosphere model would also provide the lateral heat transfer in the lower atmosphere.

Magnetic Fields

Except for some not generally accepted views on the modulation of the galactic cosmic radiation or solar phenomena by planetary bodies as seen from Earth, the only presently available experimental test for a planetary magnetic field depends either upon the detection of a synchrotron continuum, as in the case of Jupiter, or else a direct measurement at the planet.

Generally, evidence for a magnetic field should be consistent with planetary spin[8] and an internal constitution which would not inhibit convection, though a recent theory by Malkus[9] voids the requirement for spin. In any event, present radar evidence concedes, from the narrow line profile of the returned signal, a small likelihood of appreciable spin for Venus.[2] This conclusion necessarily requires the admission of

a nonspecular radar cross section at the frequencies used. Otherwise, limb contributions would be strongly suppressed. In view of the radar results, it would be surprising to find a field of low order according to dynamo theories. Higher order fields are perhaps not ruled out on the basis of Malkus' arguments. Independently of radar data, the nonexistence of a planetary field would suggest either a condition of small spin, a nominal spin and nonconvective core, or some difficulty with present views.

One finds a direct magnetic field test, then, to be an important tool in studying the relationship of the different planetary properties enumerated. This was one of the two reasons for including a magnetometer experiment; the other reason is discussed in the section on interplanetary physics.

With the Mariner magnetometer operating so that a change of about 4γ would have been seen on any of the axes, no appreciable trends above 10γ were seen nor were fluctuations like those which seem to be characteristic of the Earth's magnetospheric termination ever detected.[10] The lack of any indication of a planetary field from these data obtained on the solar side of the planet allows an upper bound to be placed upon the magnitude of the Venus dipole. A conservative view would place this value at less than 1/10 the Earth's magnetic moment if the Venus dipole were approximately normal to the ecliptic. A perhaps more accurate estimate may now be made using as an analogue the results of

Cahill and Amazeen.[11] They report a sharp boundary was observed from time to time on the sunward side of the Earth with the expected doubling of field near the subsolar termination. If this property is used for the case at hand, and a dipolar geometry is assumed, a boundary showing a discontinuity of more than 10γ is unlikely. Thus a Cytherian field of more than ~5γ is not indicated. Since the distance to the planetary center is 4.1×10^4 km, compared with the Earth's equatorial field at that distance, the Venus dipole is less than 1/20 that of the Earth, as suggested earlier. Clearly, the constraints on field multipolarity and orientation in this calculation do not rule out more complex fields.

At the same time that the magnetic field survey was under way, the array of cosmic ray apparatus was available for the detection of trapped radiation. A discussion of some of these results is given by Frank, et al.[12] Since all cosmic ray results were essentially negative, the reader is referred to the literature for details. It is important to recognize that nothing essentially different from the magnetometer results would be expected to be found by the cosmic ray detectors. The possibility remains that on future flights orbits might be made closer to planetary bodies. In this event only detailed calculation with respect to field geometries can be expected to disclose whether radiation can be trapped with sufficient stability and acceleration to make this means of detection

competitive with the more obvious use of magnetometers, the latter allowing a rather direct study of higher harmonics of the field to be undertaken in a relatively straightforward manner.

D. INTERPLANETARY EXPERIMENTS

A necessary and sufficient model for the interplanetary cavity must explain certain cosmic ray phenomena seen on Earth, such as the modulation of the galactic cosmic radiation, Forbush decreases, secular variations, and the propagation of solar cosmic rays and other debris of solar flare explosions. Central to all these problems and the construction of an appropriate model would be verification of the existence of a solar wind. Because of variability in the interplanetary medium, it may well turn out that the quiet time physics of the interplanetary cavity is fundamentally different from that which exists during times of extreme solar disturbance. The interpretation of comet observations, especially by Biermann and his group, has provided the basis for several important models. Among these, perhaps the best known is that of Parker,[13] suggesting a reasonably ordered hypersonic flow of plasma outward from the Sun. Other models, notably that of Cocconi,[14] infer a considerably more disordered outward propagation of gas. Gold's considerations have been primarily with the physical processes which take place during storm times.[15]

1. The Solar Wind

The first detection of plasma in interplanetary space is clearly assignable to the experiments of Gringanz, et al., on the Lunik flights.[16] Fluxes of 10^8 to 10^9 cm^{-2} sec^{-1} were detected with ion traps following a design of Boyd.

Mariner II is the first spacecraft to study the solar wind phenomenon over a sufficiently long period of time to remove reasonable doubts as to the general presence of such a phenomenon. With the magnetometer and the cosmic ray detectors aboard this spacecraft, it seems clear that we can now begin to lay the basis for a critical evaluation of processes which take place in the interplanetary cavity. The solar plasma detector shown in Figure 13 consists of a curved plate electrostatic analyzer of cylindrical geometry in which the deflecting force is provided by an electric field across the plates. The energy range through which the differential analyzer was swept was from 240 ev to 8400 ev in 10 steps. The detector opening was always pointed accurately toward the Sun, was sensitive to positively charged particles, had an angular acceptance of roughly 10 percent, and had energy resolution of 12 percent. The entrance slit was approximately 5 centimeters square.[5]

Plasma was seen almost continuously with this instrument; bulk velocities were from approximately 500 to 700 kilometers per

second with occasional drops or increases in these values. At times a bifurcated spectrum was noted with peaks separated generally by a factor of two in energy. Since the instrument was not designed to differentiate between different constituents having the same charge-to-mass ratio, a likely explanation suggested by the experimenters is that the upper peak was due to alpha particles. Finally, the steep angular dependence of the response requires that the data be corrected for aberration. For typical solar wind velocities this latter effect requires an increase of a factor of about two in the net flux measured.

The results of this experiment are summarized by noting that a plasma flow was always observed during the flight; it agreed in intensity with Lunik and Explorer measurements and often displayed a split or bifurcated spectrum, suggesting an alpha particle component with the same bulk velocity as the protons; and lastly, the velocity was "supersonic." The energy density found almost always exceeded that of the magnetic field;[17] the disordered or temperature energy density suggests more nearly equipartition with the field.

Velocity variability of the wind showed a 27-day periodicity and was coincident with a series of periods of enhanced geomagnetic activity (M-region storms). This is shown in Figure 14. A more detailed time resolution than that given in Figure 12 suggests to

Snyder and Neugebauer[18] that the rate of change of plasma velocity might be correlated closely with variations in the amplitude of the interplanetary field. All of this suggests the existence of variable velocity beams emitted from the Sun with a mixing interaction taking place at the juncture of adjoining streams.[19] Although the details of the general results may still be obscure, the convective supersonic model of Parker with a 1 to 2 million degree corona seems to fit the facts best.[20]

2. Magnetic Fields

Prior to the direct evidence from Pioneer V the existence of a more or less everpresent magnetic field was deduced from time variations in the galactic cosmic ray flus. From Pioneer V the presence of a steady field of ~2.5γ as a quiet time feature was ~~detected~~ deduced, though ~~and~~ the geometry of the experiment suggested that this field made a large angle with the ecliptic.[21] There were obvious difficulties in reconciling this result with the hydromagnetic requirements of a solar wind and with the propagation time features of solar cosmic rays. During this experiment, occasional interplanetary storms were also seen; special emphasis centered about the March 30 - April 1, 1960 events.[22]

Turning to the Mariner ~~experiment~~ flight, the geometry used for the magnetometer experiment is shown in Figure 15. The symbols X, Y, and Z define a mutually orthogonal system of unit vectors with Z pointing away from the Sun and being directed along the roll axis

of the spacecraft. The plane defined by the axes Y and Z intersects the Earth by virtue of the Earth tracker which rolls the spacecraft into such a position as to always track the Earth along this direction. X then is defined as the remaining mutually orthogonal vector in a left handed sense. Therefore, in a heliocentric system, Z points along the radial component of the interplanetary magnetic field, and the plane defined by the unit vectors X and Y contains the other two components of the field. The immediate postlaunch phase of the voyage of Mariner II included a residual rate of roll of the spacecraft introduced by the launching process. Thus a steady interplanetary magnetic field should have displayed a sinusoidal variation for the sensors X and Y. The rolling cycle was utilized for calibration of the X and Y sensors. The Z axis component of the field cannot, however, be known absolutely by this means and other procedures are being explored. Preliminary analysis of the magnetometer data indicates that one of the most important results is the convincing evidence that interplanetary space is rarely empty or field free.[23] Magnetic fields of at least a few gamma are nearly always present except, perhaps, for occasional transient nulls as shown in Figure 16. Here φ is the angle defined by the arctangent of the ratio of the X and Y components, thus indicating the angle the transverse component of the field makes with the ecliptic. The magnitude of the field component along

the X and Y directions agrees reasonably well with the Pioneer V observations. The magnitude is typically 5 gamma during times of small magnetic activity, often making a substantial angle with the ecliptic, rising to values of 20 gamma or more during magnetic storms, and falling to about 2 gamma during very quiet times.

A number of magnetic storms took place during the flight of Mariner II. Figure 17 illustrates the more or less repeated behavior of the plasma stream during such times. It is generally true that the energy at peak flux shifts to higher levels during times of disturbance as can be seen on this diagram. It is clear then that the ordered energy density of the solar wind does increase during times of geomagnetic disturbance. However, the plasma volume density, at least for these storms, never reaches values suggested by earlier investigations and simple models of either the undisturbed or disturbed time interplanetary magnetic field do not provide a clear relation to the data.

Two different storm events that occurred during the flight have been examined in more detail.* The storm of October 7, 1962 (fig. 18) is listed as a gradual commencement event, though earlier listings proposed a sudden commencement. The initial phase was

---

*The field values quoted here must, at the time of this writing, be taken as tentative and subject to correction, though it is not thought that the gross features are likely to change by much if corrected.

strong and the main phase degenerate. College showed little storm effect during this period. During this time Mariner II was ~0.06 AU from the Earth approximately on the line joining the Earth and Sun.

The primary character of the interplanetary medium is assigned by analysis of the magnetometer and plasma data, the latter of which has been summarized by Snyder and Neugebauer. The most prominent features of the plasma data are given in Figure 19 which is a photograph of a model of both plasma and field for the initial two hours encompassing the beginning of the interplanetary disturbance. The initial activity consisted of a decrease to an undetectable limit of channel 3 (520 ev/Z) of the plasma probe, together with changes in channels 4, 5, and 6 (generally increases in flux) and a switching on of channel 7. All these events occurred during one data frame of the plasma probe (~3.5 minutes). Simultaneously with the plasma change the magnetic field, shown in Figure 20, displayed a pulse-like rise from ~7 to 16γ immediately followed by a partial relaxation to about 10γ which, in turn, was followed by many hours of turbulent fields. A summary of this storm for a period of 32 hours is given in Figure 21.

The conclusions of these data are that the solar cloud causing the storm of October 7, 1962 was led by a shock wave of strength ~2 and that the shock may have been strongly oblique and was associated with an increase in gas temperature.

The implications from this storm are that the solar gas pressing outward into the solar system originated on the Sun in a region lying to the south of the ecliptic plane. Since in October the north pole of the Sun nearly points to the Earth, it is not possible to assign the disturbance to a southerly solar latitude. It is suggested, however, that since the shock normal was northward with respect to the ecliptic plane and pointed in the direction of the Earth's velocity, the solar gas or blast gas traveled mainly below and under the Earth and struck the planet a glancing blow sufficient to cause a strong sudden commencement and initial phase but insufficient to immerse the Earth in a plasma cloud deeply enough to produce the expected main phase decrease. Arguments based on an M region beam rotating with the Sun and striking successively the spacecraft and Earth would not be likely to display the transit time pattern measured but cannot be completely ruled out at this time.

The interplanetary disturbance for September 11, 1962 is considerably more difficult to identify. Although the Earth storm starts at 0520 GMT, no shock is identifiable in space from 00 hr to 0300 and is therefore presumed absent. Tentative identification of the disturbance begins at 0106 GMT, from the plasma data which show a sudden jump in flux by a factor of 6.5 with little or no heating. The attendant field measurements are shown in Figure 22, the field

showing a small decline in amplitude from ~9γ to ~6γ continuing to point northward (normal to the ecliptic). The ordered plasma velocity is 460 ±40 km/sec. The plasma volume density varies over one order from ~0.3 to 3 cm^{-3} during this time. Thus the Alfvén velocity was ~10^8 cm/sec for a field of 9γ and the sound velocity ~100 km/sec. Clearly, in the frame of the moving gas, the plasma density gradient moves at a subsonic or sub-Alfvén velocity. Thus the view is tentatively adopted that for this storm the gas cloud is propagating with a shockless transition layer ahead. In view of the expected r^{-2} dependence of both field and plasma density, it seems likely, if the Alfvén velocity were the dominant factor in determining the Mach number, that a shock had never existed.

3. Cosmic Rays

Mariner is especially well adapted to the survey of cosmic radiation en route to Venus, because of the variation in range from 1 AU inward to 0.7 AU. During the flight from Earth to Venus, the Sun completed nearly four revolutions, the spacecraft traversed more than 1/4 the distance around the solar system while nearly continuous flux measurements were made. The sun was in the waning part of the solar cycle and thus it was reasonable to expect that the more obvious aspects of solar activity might be suppressed. Nevertheless, the occurrence of M-type storms, the presence of low-energy particles, time variations in the galactic flux, and the ~~quest~~ search for a

radial gradient appeared to be reasonable kinds of effects to investigate. This is especially true when viewed from the standpoint of the lack of any prior survey over as extended a time or distance in interplanetary space. A by-product of cosmic-ray survey experiments is indicated by the close approach to Venus allowing a test to be made for trapped radiation. In this instance, the evidence for a magnetic field is perhaps more indirect than it would be with a magnetometer since a complex field not especially suitable for stable trapping might still be present. Nevertheless, such a quest has the appeal of simplicity if detectability alone is the primary criterion.

In view of the limited scientific payload, simple and rugged counting equipment was chosen for cosmic ray detection. Reference to table I shows the total complement of cosmic ray counters. The ion chamber was of the integrating pulse Neher design, making of it basically a total charge integrating detector. One of the GM tubes was shielded with absorber of thickness equal to that of the ion chamber (0.2 gm/cm^2). Ion chamber wall material was stainless steel as was most (0.16 gm/cm^2) of one of the GM tubes. A second tube, although of the same absorber thickness, was primarily Be. The intent was to differentiate between electrons and heavy particles by the strong radiative collision effect (Bremsstrahling) and approximately Z^2 dependence for electrons. The effect will necessarily be mixed with general spacecraft Bremsstrahling and therefore

be somewhat complicated. The third GM tube was of the thin-end window variety; window thickness was 7.2 mgm/cm^2 admitting electrons of energy greater than 40 kv. Since the proton threshold is 0.5 mev for this window, especial interest centers on this detector.

HAO preliminary reports for the flight period of Mariner indicate six class 2 flares (24 August to 8 November). Only 23 October and 7 September were associated with Type IV bursts. The latter event was east limb and not seen by the high-energy detectors. The 23 October event has been reported upon by Anderson[24] and Neher and suggests a more or less classic solar cosmic ray event with mean specific ionization of ~1200. Decay followed a set of three successive first-order decays characterized by assignable time constants.

The 213 GM tube is reported[25] as having registered a base level of ~1 sec^{-1} corresponding to ~5 cm^{-2} sec^{-1}. The somewhat higher rate than that reported by earlier deep space measurements may be attributable to the suppression of the low-energy tail of the galactic flux during times of higher solar activity, to detection of lower energy primaries due to the better counter response in the present instance, or to some other effect. Bursts of radiation lasting typically a day or longer were seen by the 213 counter on several occasions coincident with increased interplanetary activity. Only for the October 23 events did all counters respond and in that instance, as mentioned earlier, at least heavy particles of solar origin are suggested by the high mean

specific ionization. In the other instances, since little other than a galactic background is suggested by the high-energy counters, it is tempting to consider the nature of the enhancement of the 213 rate. Even on October 23, the increase from the base level of ~5 cm^2 sec^{-1} to ~500 cm^{-2} sec^{-1} compared to the rate of 10-15 cm^{-2} sec^{-1} observed by Anderson and Neher suggests a strong flux of lower energy particles. Whether these are electrons, ions, or both, cannot be told clearly. The argument for electrons would rest upon the Bremsstrahling aspects of the data. From the limited information available at the time of this writing the apparent lack of any appreciable response at times other than October 23 would suggest heavy particles as the source of the burst radiation seen by the 213 counter. An investigation of riometer data for this period might shed light on whether the 213 events are related to PCA's. Also, Anderson and Neher report little, if any, galactic gradient for the period of 31 August to 15 November.

4. Micrometeorites

Lastly, an important observation made by the cosmic dust experiment on Mariner II deserves comment. The small particle flux indicated was some two orders of magnitude less than that reported by Dubin from Pioneer I, which in turn was considerably less than those reported by satellites. Thus it appears that the hypothesis of a concentration of small dust particles near the Earth is substantiated. Unfortunately,

temperature problems caused a malfunction of the micrometeorite experiment in the vicinity of Venus. A negative finding for that planet would have lent support to the model where cislunar dust is created partially by secondary splash from hypervelocity cratering of primary objects upon the Moon.

Acknowledgement

The author expresses appreciation to the various scientists who have discussed material prior to publication and particularly to L. D. Kaplan, G. Neugebauer, and H. Anderson for extended discussions.

BIBLIOGRAPHY

1. Murray, Bruce C., Wildey, Robert L., and Westphal, James A.: 1963, Infrared Photometric Mapping of Venus Through the 8- to 14-Micron Atmospheric Window. J.G.R. 68, 4813.

2. Goldstein, R. M., and Carpenter, R. L.: 1963, Goldstone Radar Observations of Venus During 1962. Science 139, 910.

3. See Mariner Mission to Venus, JPL staff, McGraw Hill (1963) for a complete semitechnical account of the whole mission.

4. A more complete summary of instrument details is given in JPL Tech. Rep. 32-315, Scientific Experiments for Mariner R-1 and R-2 (July 1962). (Performance is not included as publication of this document was prior to launch.)

5. Mariner II: Preliminary Reports on Measurements of Venus, 1963, Science 139, 905-910. This series consists of four papers which will be subsequently referenced in abbreviated form, for example, this reference by Barath, F. T., Barrett, A. H., Copeland, J., Jones, D. E., and Lilly, A. E., p. 908.

6. Mariner II: Venus. Chase, S. C., Kaplan, L. D., and Neugebauer, G.: 1963, Science 139, 907.

7. Chase, S. C., Kaplan, L. D., and Neugebauer, G.: The Mariner II Infrared Radiometer Experiment. In press.

8. Inglis, D. R.: 1955, Theories of the Earth's Magnetism. Rev. Mod. Phys., 27, 212.

9. Malkus, W. V. R.: 1963, Precessional Torques as the Cause of Geomagnetism. J. Geophys. Research 68, 2871.

10. Mariner II: Venus. Coleman, P. J., Davis, L., Jr., Smith, E. J., and Sonett, C. P.: 1963, Science 139, 909.

11. Cahill, L. J., and Amazeen, P. G.: 1962, The Boundary of the Geomagnetic Field. Univ. New Hampshire Rep. 62-1.

12. Mariner II: Venus. Frank, L. A., Van Allen, J. A., and Hills, H. K.: 1963, Science 139, 905.

13. Parker, E. N.: 1958, Dynamics of the Interplanetary Gas and Magnetic Fields. Ap. J., 128, 667.

14. Cocconi, G., Gold, T., Areisen, K., Hayakawa, S., and Morrison, P.: 1957, UPAP Cosmic Ray Conf., Varenna.

15. Gold, T.: 1959, Plasmas and Magnetic Fields in the Solar System. J. Geophys. Research 64, 1665.

16. Gringauz, K. I., Bezrukikh, V. V., Ozerov, V. D. and Rybchinskiy, R. Ye: 1961, Study of the Interplanetary Ionized Gas, High Energy Electrons, and Solar Corpuscular Radiation by Means of Three Electrode Traps for Charged Particles on the Second Soviet Cosmic Rocket. Artificial Earth Satellites, vol. 6, Moscow.

17. The Mission of Mariner II: Preliminary Observations. This is the counterpart series to reference 3 and will, for brevity, be dealt with in the same manner. Thus the present reference is Neugebauer, M., and Snyder, C. W.: 1962, Science 138, 1095.

18. Snyder, C. W., and Neugebauer, M.: 1963, Interplanetary Solar Wind Measurements. COSPAR Symposium, Warsaw.

19. Davis, L.: 1962, The Effect of Solar Disturbances and the Galactic Magnetic Field on the Interplanetary Gas. J. Phys. Soc., Japan, 17, Supp. A-II, 543.

20. Parker, E. N.: 1960, Ap. J., 132, 821.

21. Coleman, P. J., Davis, L., and Sonett, C. P.: 1960, The Steady Component of the Interplanetary Field. Phys. Rev. Lett., 5, 43.

22. Coleman, P. J., Sonett, C. P., and Davis, L.: 1961, On the Interplanetary Magnetic Storm: Pioneer V. J. Geophys. Res., 66, 2043.

23. Mariner II: Preliminary Observations. Coleman, P. J., Davis, L., Smith, E. J., and Sonett, C. P.: 1963, Science 138, 1099.

24. Anderson, H. R.: The Mariner II High Energy Radiation Experiment - preprint.

25. Mariner II: Preliminary Observations. Van Allen, J. A., and Frank, L. A.: 1962, Science 138, 1098.

TABLE I.- MARINER R SCIENTIFIC INSTRUMENT WEIGHTS AND ELECTRICAL POWER REQUIREMENTS

Experiment	Weight, pounds	Maximum electrical power requirement, watts
Microwave radiometer	21.87	8.9
Infrared radiometer	2.67	2.1
Magnetometer	4.66	6.0
Charged particle flux detectors	2.78	0.4
Cosmic dust detector	1.85	.08
Solar plasma analyzer	4.80	1.0
Data conditioning system	6.41	2.01
Power Switching	1.68	.58
Scan actuator	2.88*	2.5
	46.72	23.57

*Not included in scientific instrument package weight.

(from ref. 2)

TABLE II

			Purpose
Microwave Radiometer	A. H. Barrett D. E. Jones J. Copeland A. F. Lilley	λ = 13.5 mm; 19 mm crystal video detector beam $\theta = 2.2^{\circ}; 2.5^{\circ}$ angular scan rates: search mode 1 deg/sec meas. mode 0.1 deg/sec	Center-limb brightening or darkening; phase effects 19mm surface "temp" H_2O abs. at 13.5 mm
Infrared radiometer	L. D. Kaplan G. Neugebauer C. Sagan	λ = 8.5μ, 10.4μ thermistor bolometers $\Delta\theta \sim 0.9^{\circ}$ scan modes and rates same as microwave radiometer	Cloud top vs. mixed atm. depth source of IR temperature; center-link variation
Magnetometer	P. J. Coleman, Jr. L. E. Davis, Jr. E. J. Smith C. P. Sonett	Triaxial flux gate	Planetary magnetic field; general properties of collision-free interplanetary plasma; long term behavior of large-scale interplanetary field behavior
Ion chamber Geiger-Muller tube array	H. R. Anderson H. V. Neher	0.2 gm/cm^2 steel (ion chamber. 0.03 gm/cm^2 glass plus 0.16 gm/cm^2 steel (GM no. 1). 0.03 gm/cm^2 glass plus 0.113 gm/cm^2 Be (GM no. 2). proton threshold 10 mev β^- direct threshold 0.5 mev	Radial solar dependence of galactic and solar cosmic rays; time variations, Venus trapped radiation. Be steel difference to separate β^- and heavies.
Thin-window GM tube	J. A. Van Allen	1.2 mgm/cm^2 mica window half angle of 45°; axis 70° from sun line	Venus trapped radiation; interplanetary energetic radiation
Plasma probe	C. W. Snyder M. Neugebauer	Electrostatic analyzer 240 ev/Z - 8400 ev/Z	Detect solar wind study properties of collision-free interplanetary plasma

TABLE III. - Radiometer Characteristics

Item and unit	Channel	
	1	2
Center wavelength (mm)	19	13.5
Center frequency (Gcy/sec)*	15.8	22.2
Predetection bandwidth (Gcy/sec)*	1.5	2.0
Sensitivity, rms (^{o}K)	15	15
Calibration signals (^{o}K)	1500	800
Time constant (sec)	40	40
Beam width (deg)	2.5	2.2
Side lobes (db)	-23	-23
Reference frequency (Cy/sec)	950	1050

*1 Gcy = 10^{9} cycles.

(from ref. 3)

FIGURE LEGENDS

Figure 1.- Mariner II at lift-off. At this moment began actual exploration of the planets (NASA photograph).

Figure 2.- The Mariner R spacecraft. This vehicle was redesignated Mariner II. The photograph is of a model used for clarity in demonstrating the equipment positions (NASA photograph).

Figure 3.- Ecliptic view of Mariner II and Pioneer V showing the interplanetary juxtaposition of orbits.

Figure 4.- Burning and acquisition of the Mariner system shown in schematic sequence. The portion of the near-Earth trajectory from 6 to 7 is a portion of an ellipse and represents the coast period from the end of Agena first burn until intersection with the optimum firing point for launch into interplanetary orbit.

Figure 5.- The midcourse maneuver. The object is to trim the total velocity vector after determination of the "velocity to be added" error resulting from Agena second burn residual errors. Since the spacecraft motor has a nozzle fixed along the roll or symmetry axis of the spacecraft, the vector increment requires a predetermined attitude of the spacecraft obtained by roll and pitch maneuvers. Then the spacecraft is returned to nominal interplanetary configuration.

Figure 6.- Encounter geometry showing the point of closest approach or impact parameter.

Figure 7.- View of Venus during scan with coordinate system determined by planetary equator defined by ecliptic plane. Scans were made while at southerly Venus latitudes favoring southern hemisphere scans.

Figure 8.- Microwave radiometer data showing approximately symmetric limb darkening for scans 1 and 3. (Courtesy of Chase, et al.)

Figure 9.- Schematic of the infrared radiometer. Space reference was used for the synchronous detector and a metal plate for calibration as discussed in text. (Courtesy of Chase, et al.)

Figure 10.- Filter pass-band characteristics for IR scanners (from JPL TN 32-315).

Figure 11.- Beam width of 8μ IR channel. (Courtesy of Chase, et al.)

Figure 12.- IR signals from scan of Venus. Nearly symmetric limb darkening is evident in this plot.

Figure 13.- Electrostatic analyzer for study of solar wind. Aperture is at lift bottom and is mounted to point accurately at Sun (from JPL TN 32-315).

Figure 14.- Kp-plasma daily average velocity with strong correlation. A and C notation refer to repetitive storm phenomena (from Snyder and Neugebauer).

Figure 15.- Coordinate system for magnetometer.

Figure 16.- "Daily" variation of magnitude and direction of interplanetary field during early phase of flight. Fluctuating "out of ecliptic" component is clear from variation of φ, angle between ecliptic and field (from Coleman, et al.).

Figure 17.- Relation of plasma velocity at peak flux and storms as seen on Earth.

Figure 18.- Gradual commencement geomagnetic storm of October 7-9 showing a degenerate main phase.

Figure 19.- Tentative model of interplanetary disturbance of October 7, 1962. The initial shock is identified by the plasma change and its collision-free aspects by the field pulse. The tangled fields following are characteristic of the subsequent many hours.

Figure 20.- Plan, elevation, and amplitude of interplanetary fields for October 7. These data are tentative and subject to correction though the gross aspects are thought to be a reflection of the actual field.

Figure 21.- Summary of the October 7-9 storm showing both field and plasma averages.

Figure 22.- Time period thought to be associated with the large geomagnetic storm of September 11, 1962. Plasma changes are moderate and no shock is detectable. Field orientation appears to be the primary identifiable characteristic. Again as in Figure 20, the field values are preliminary and subject to revision.

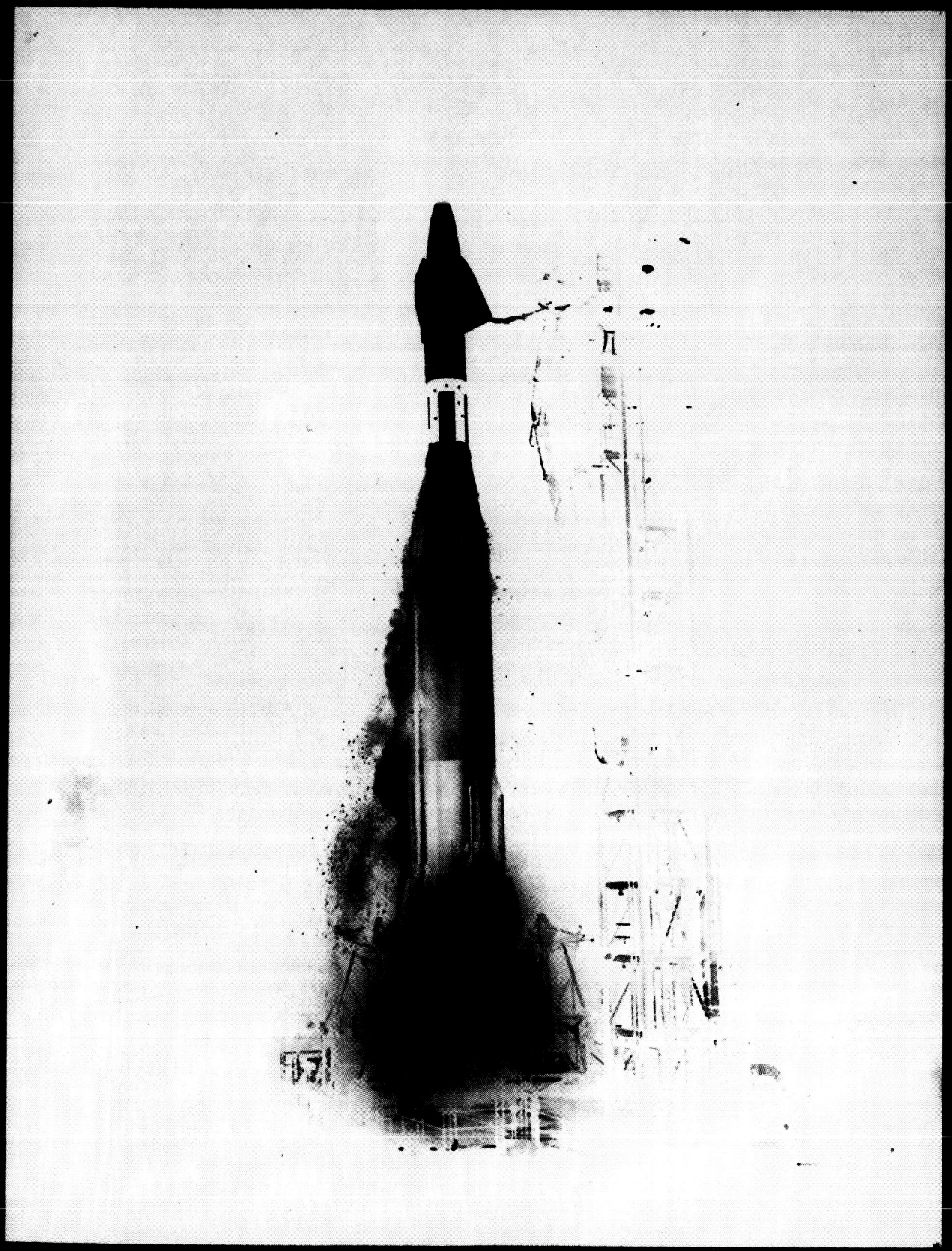

Figure 1.

NATIONAL AERONAUTICS AND SPACE ADMINISTRATION
AMES RESEARCH CENTER, MOFFETT FIELD, CALIFORNIA

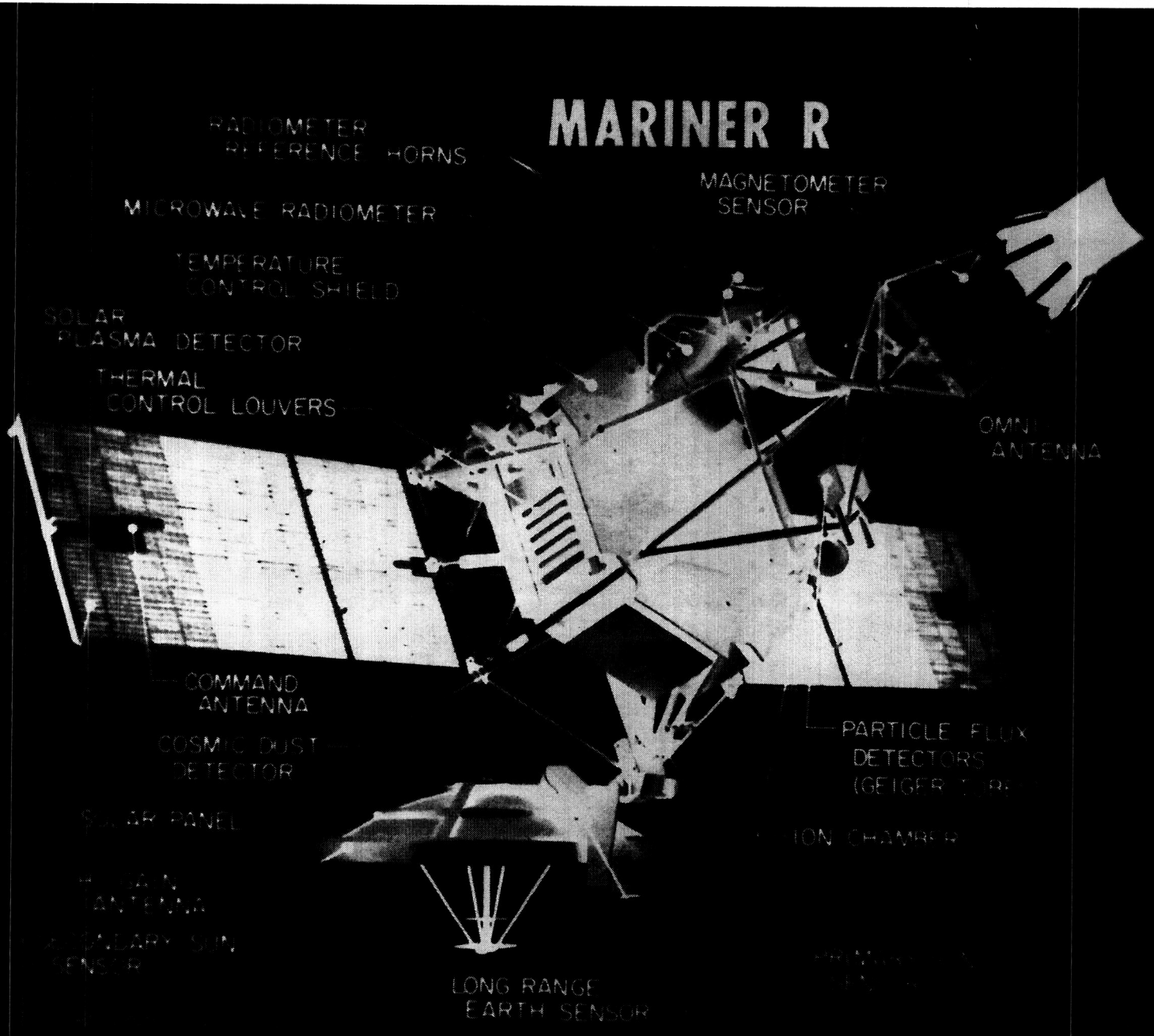

Figure 2.

NATIONAL AERONAUTICS AND SPACE ADMINISTRATION
AMES RESEARCH CENTER, MOFFETT FIELD, CALIFORNIA

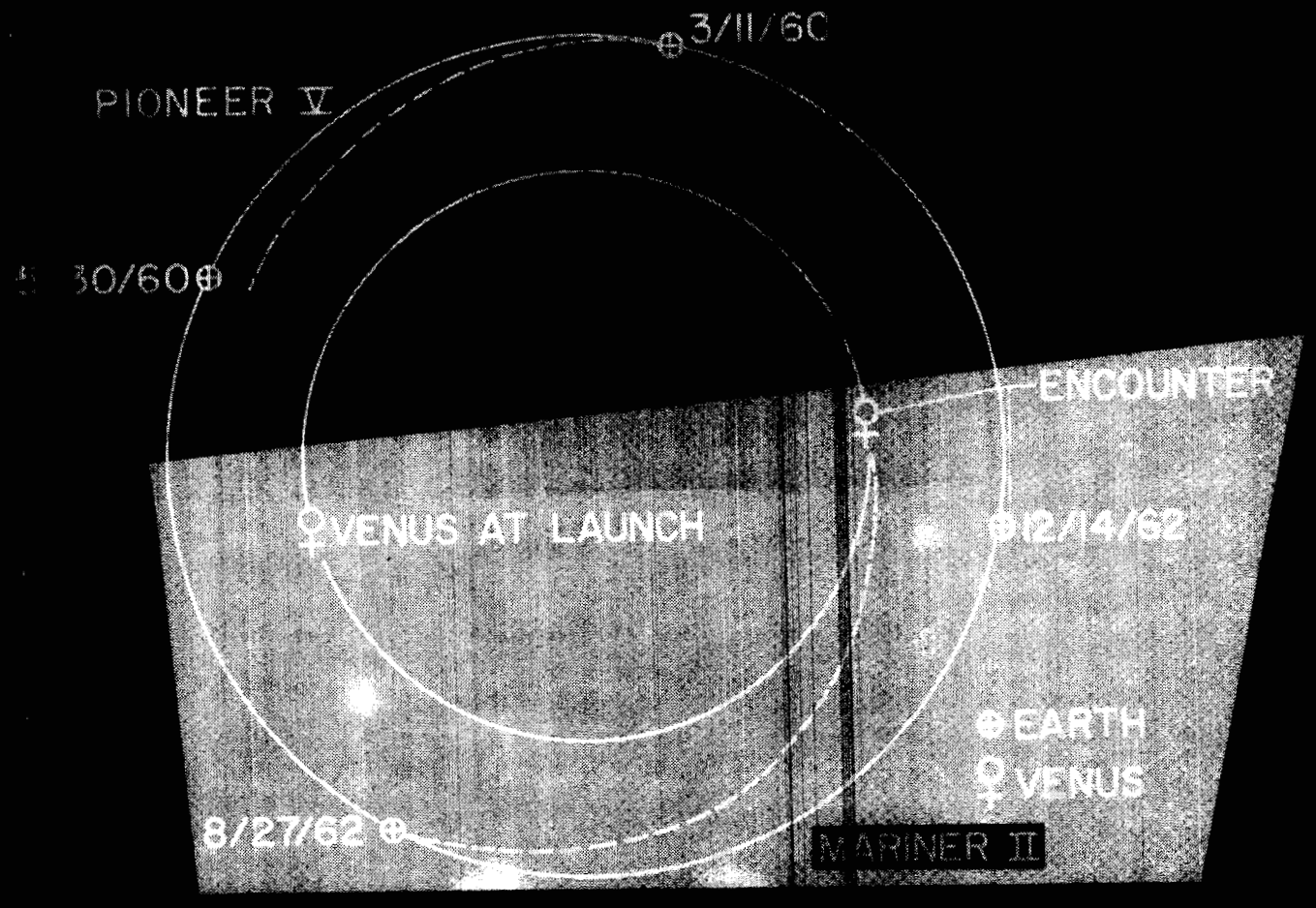
3/11/60
PIONEER V
5/30/60
ENCOUNTER
VENUS AT LAUNCH
12/14/62
EARTH
VENUS
8/27/62
MARINER II

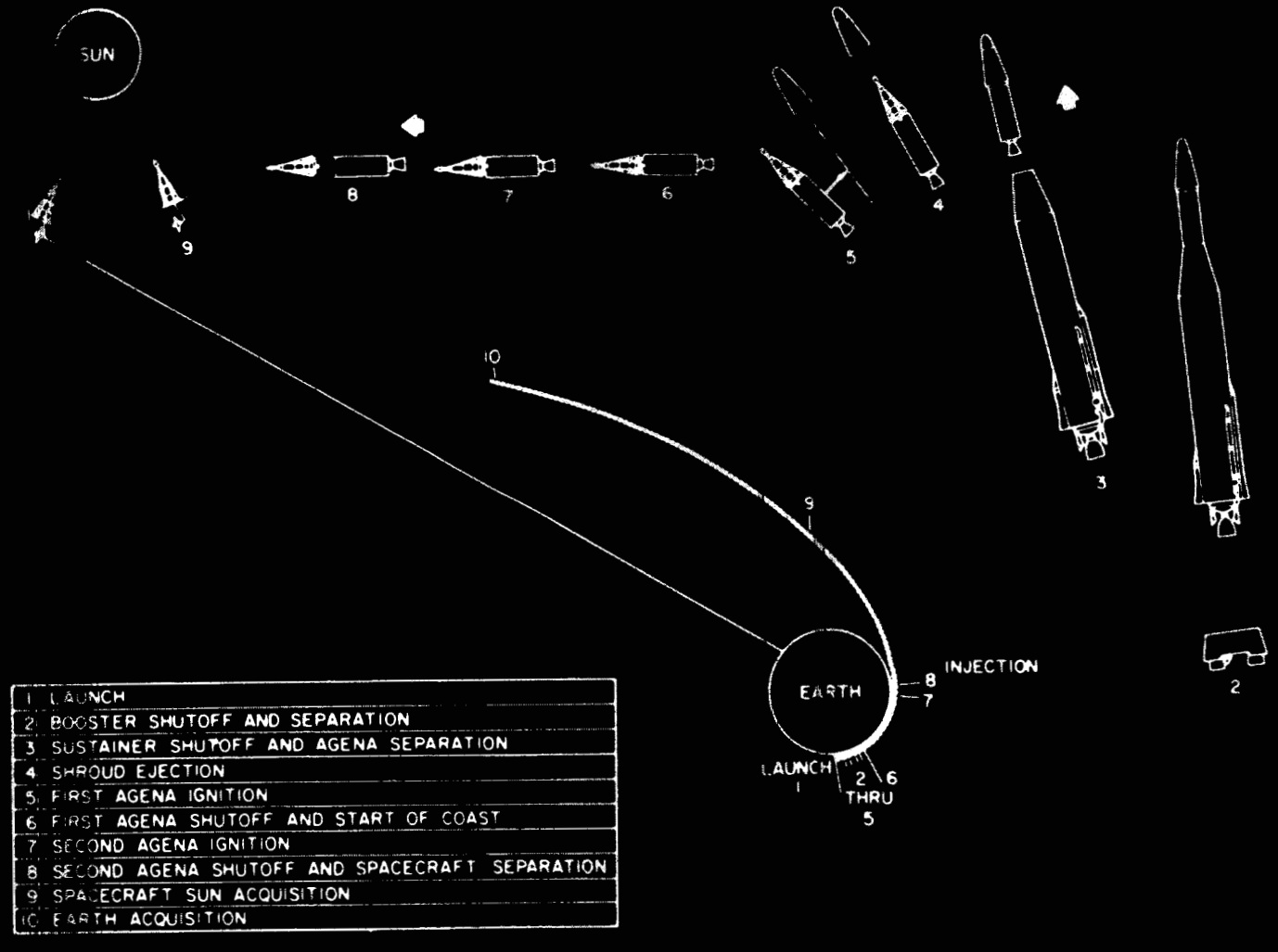

Figure 4.

NATIONAL AERONAUTICS AND SPACE ADMINISTRATION
AMES RESEARCH CENTER, MOFFETT FIELD, CALIFORNIA

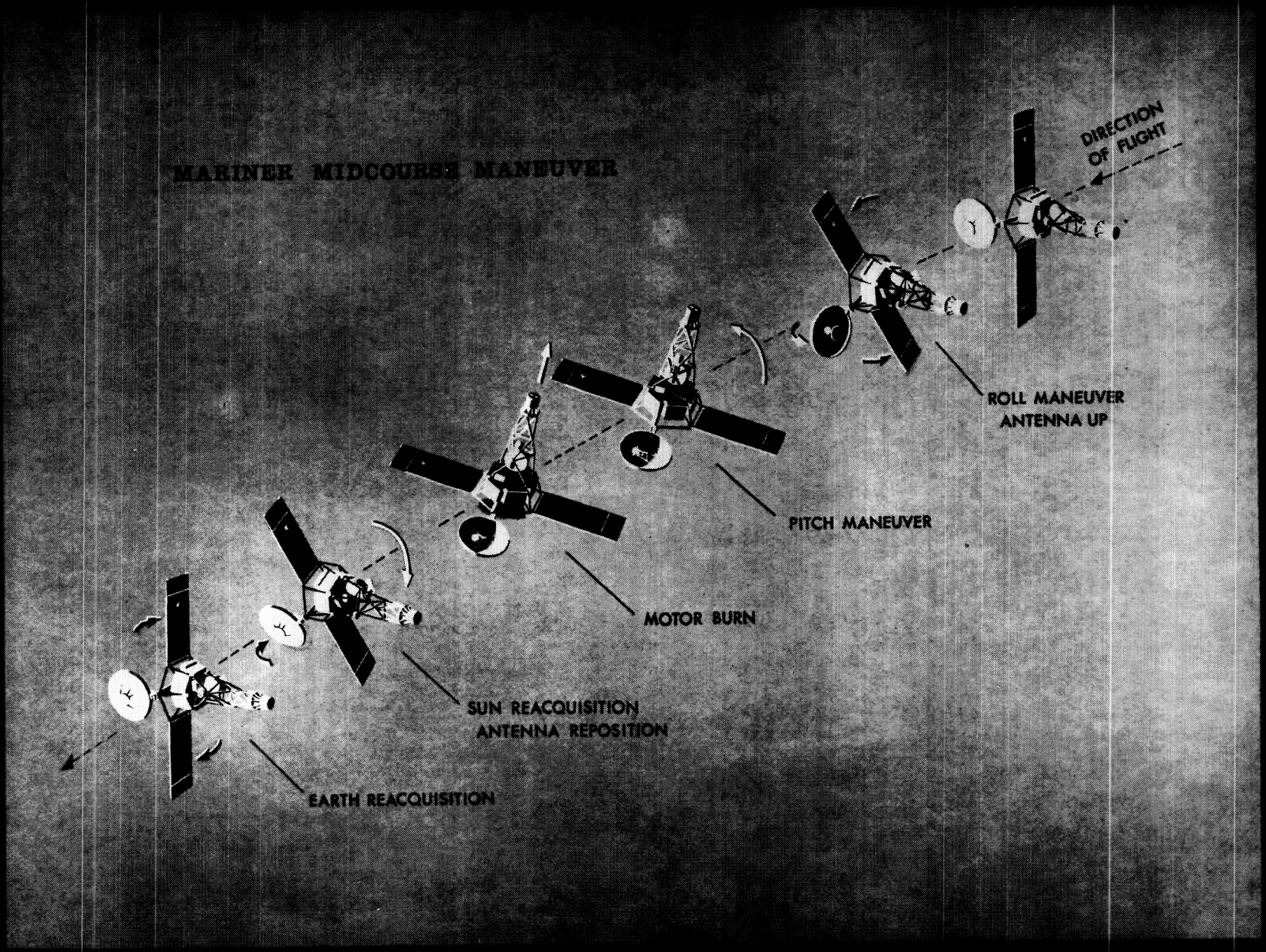

Figure 5.

NATIONAL AERONAUTICS AND SPACE ADMINISTRATION
AMES RESEARCH CENTER, MOFFETT FIELD, CALIFORNIA

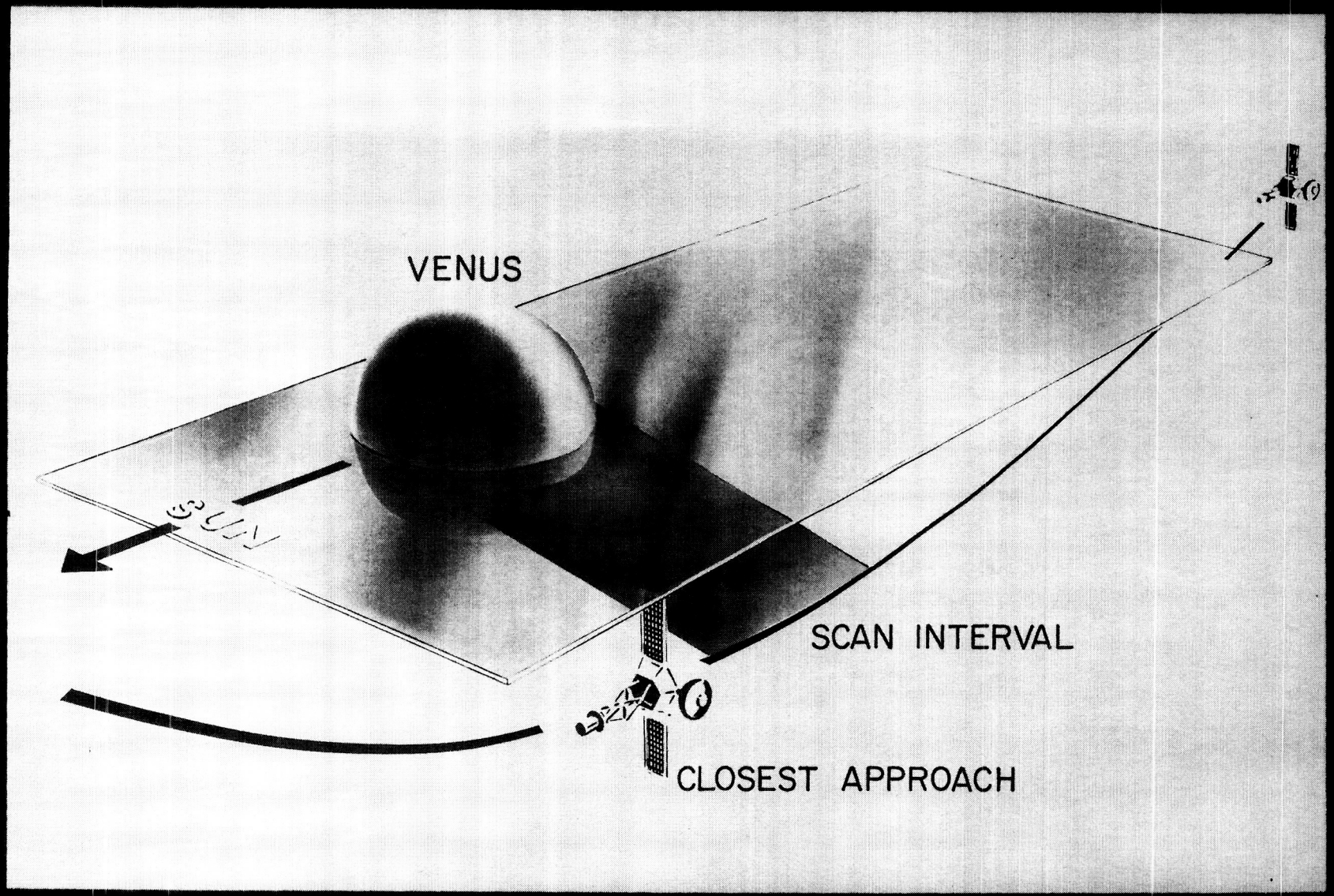

Figure 6.

NATIONAL AERONAUTICS AND SPACE ADMINISTERATION
AMES RESEARCH CENTER, MOFFETT FIELD, CALIFORNIA

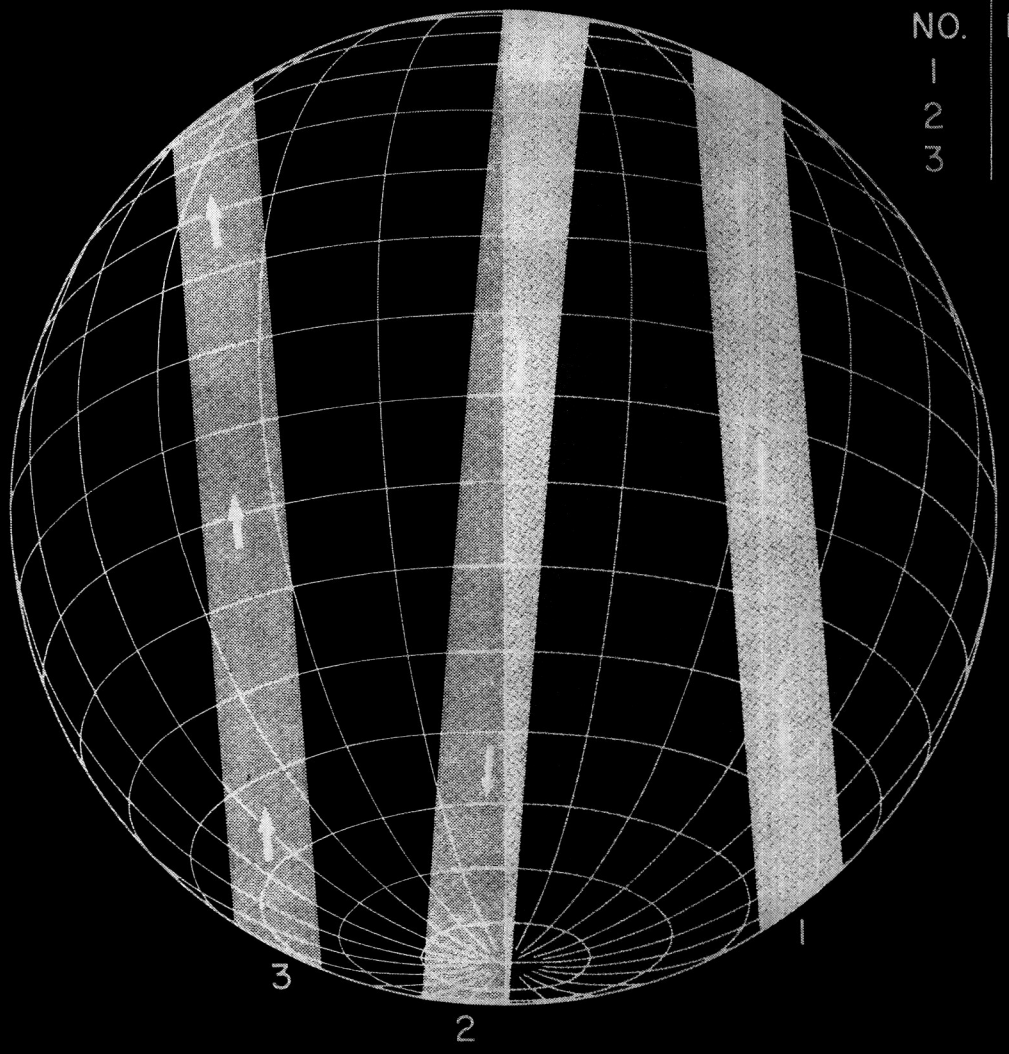

SCAN NO.	NO. READINGS	START TIME
1	~ 7	1902 Z
2	~ 10	1916.5Z
3	~ 10	1934 Z

Figure 7.

NATIONAL AERONAUTICS AND SPACE ADMINISTRATION
AMES RESEARCH CENTER, MOFFETT FIELD, CALIFORNIA

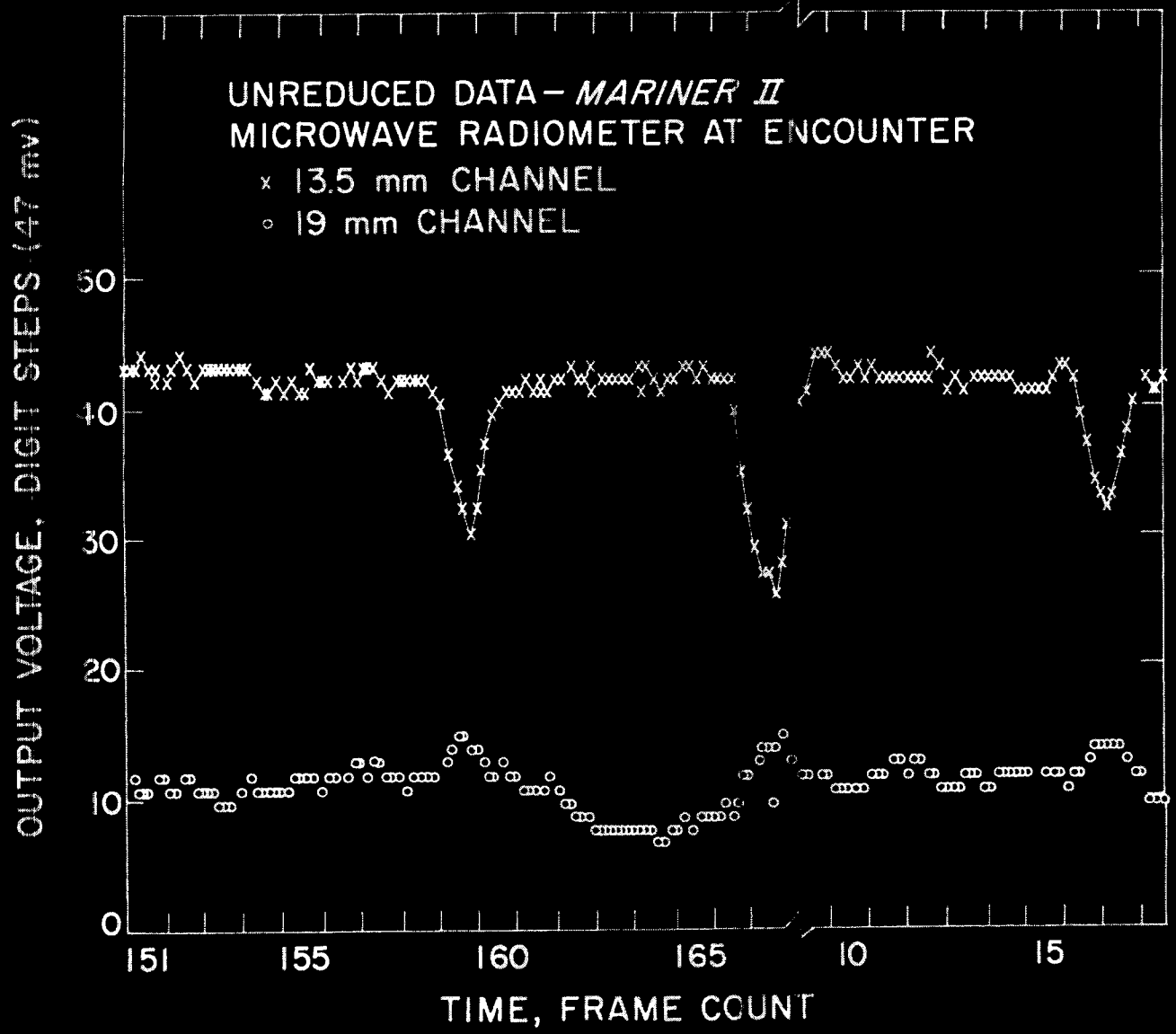

Figure 8.

NATIONAL AERONAUTICS AND SPACE ADMINISTRATION
AMES RESEARCH CENTER, MOFFETT FIELD, CALIFORNIA

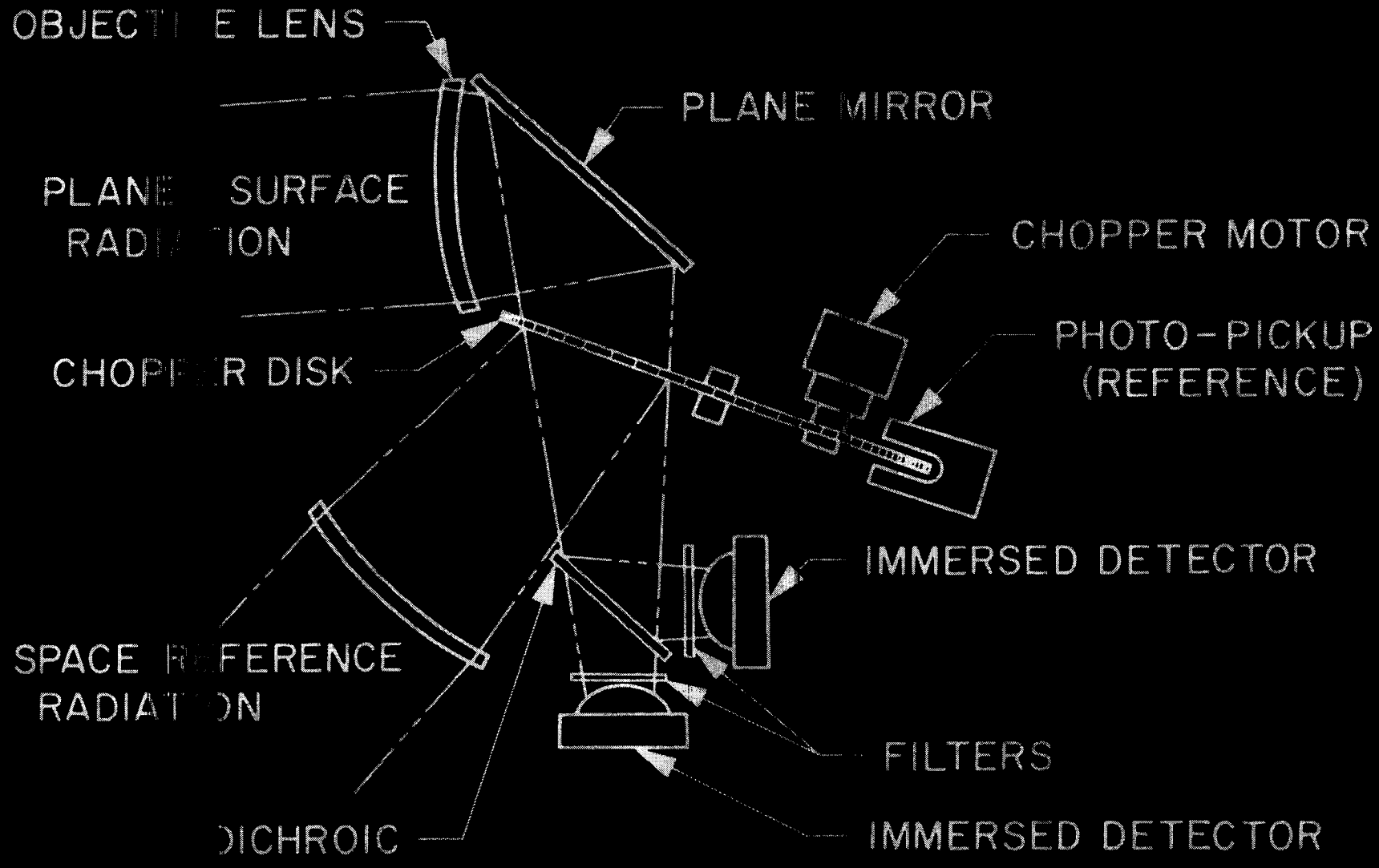
OBJECTIVE LENS
PLANE MIRROR
PLANE SURFACE
RADIATION
CHOPPER MOTOR
CHOPPER DISK
PHOTO-PICKUP
(REFERENCE)
IMMERSED DETECTOR
SPACE REFERENCE
RADIATION
FILTERS
DICHROIC
IMMERSED DETECTOR

Figure 2.

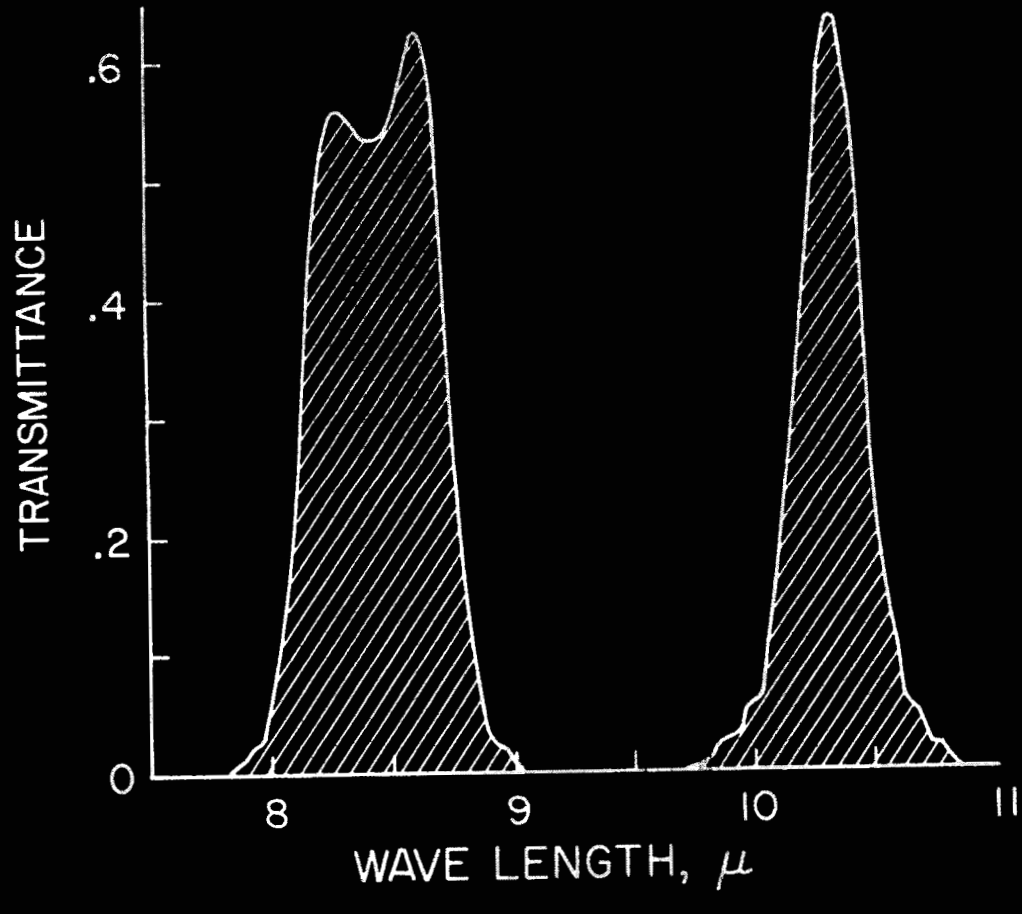

Figure 10.

NATIONAL AERONAUTICS AND SPACE ADMINISTRATION
AMES RESEARCH CENTER, MOFFETT FIELD, CALIFORNIA

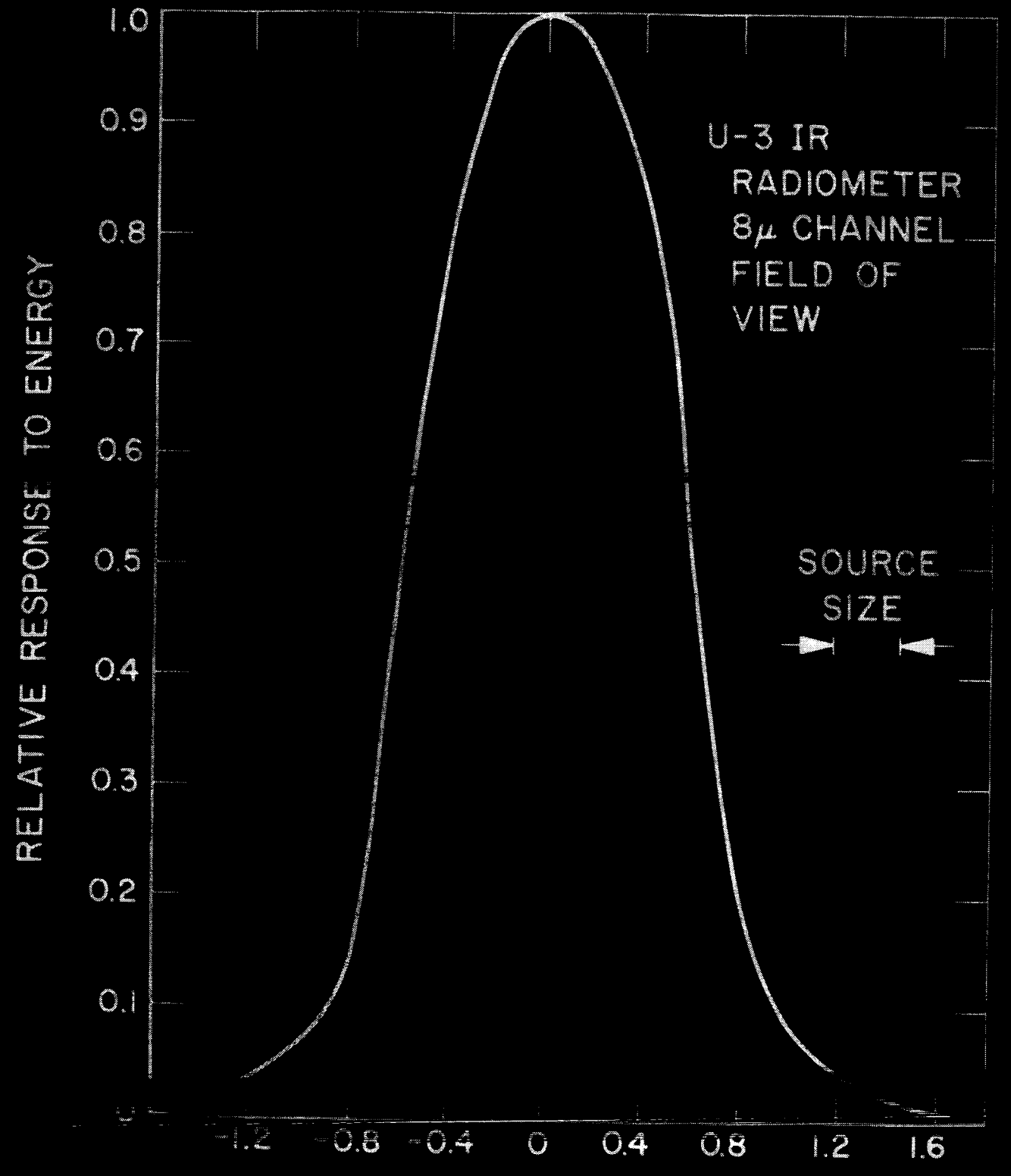
RELATIVE RESPONSE TO ENERGY
1.0
0.9
0.8
0.7
0.6
0.5
0.4
0.3
0.2
0.1
0
-1.2
-0.8
-0.4
0
0.4
0.8
1.2
1.6
U-3 IR
RADIOMETER
8μ CHANNEL
FIELD OF
VIEW
SOURCE
SIZE

Figure 11.

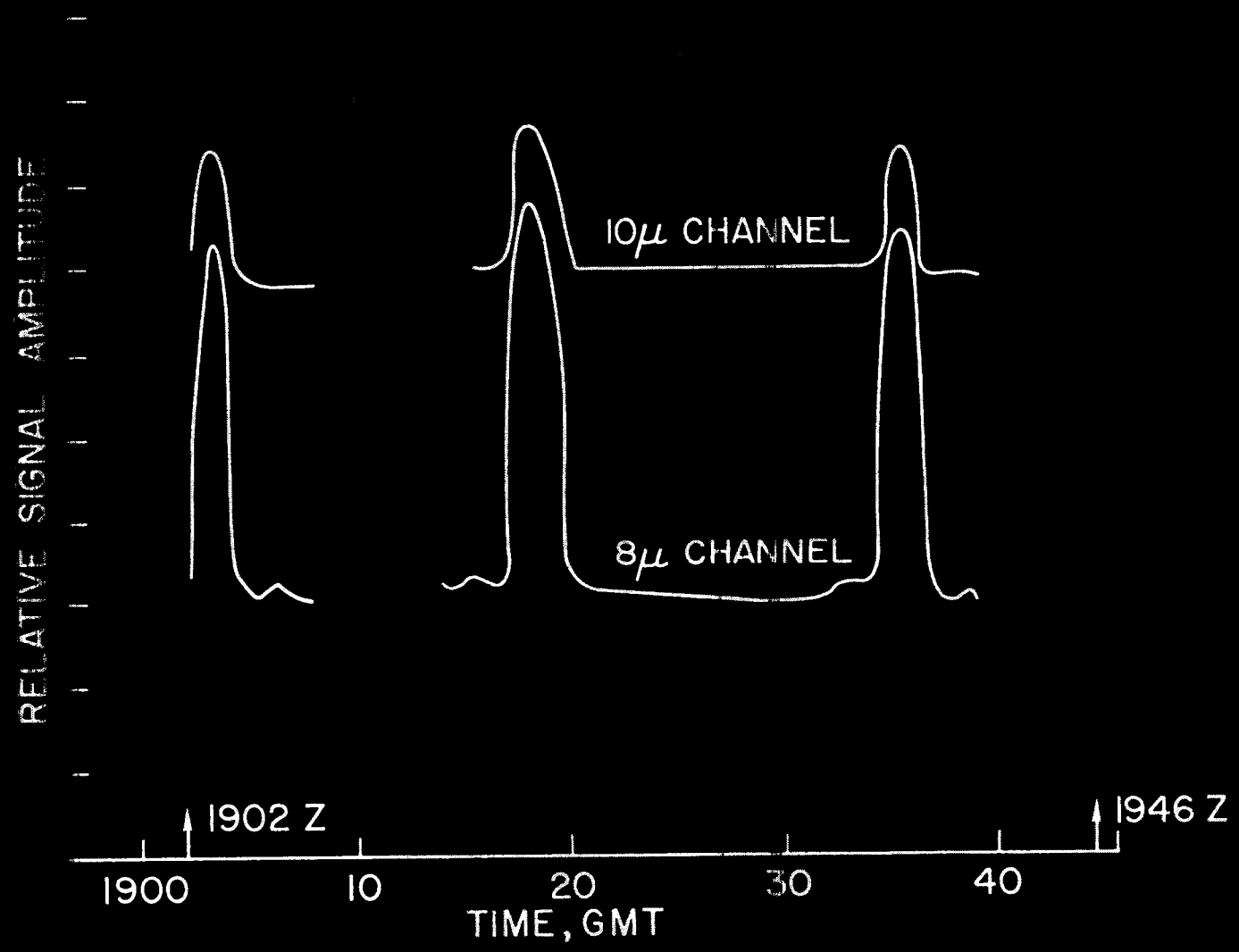

Figure 12.

NATIONAL AERONAUTICS AND SPACE ADMINISTRATION
AMES RESEARCH CENTER, MOFFETT FIELD, CALIFORNIA

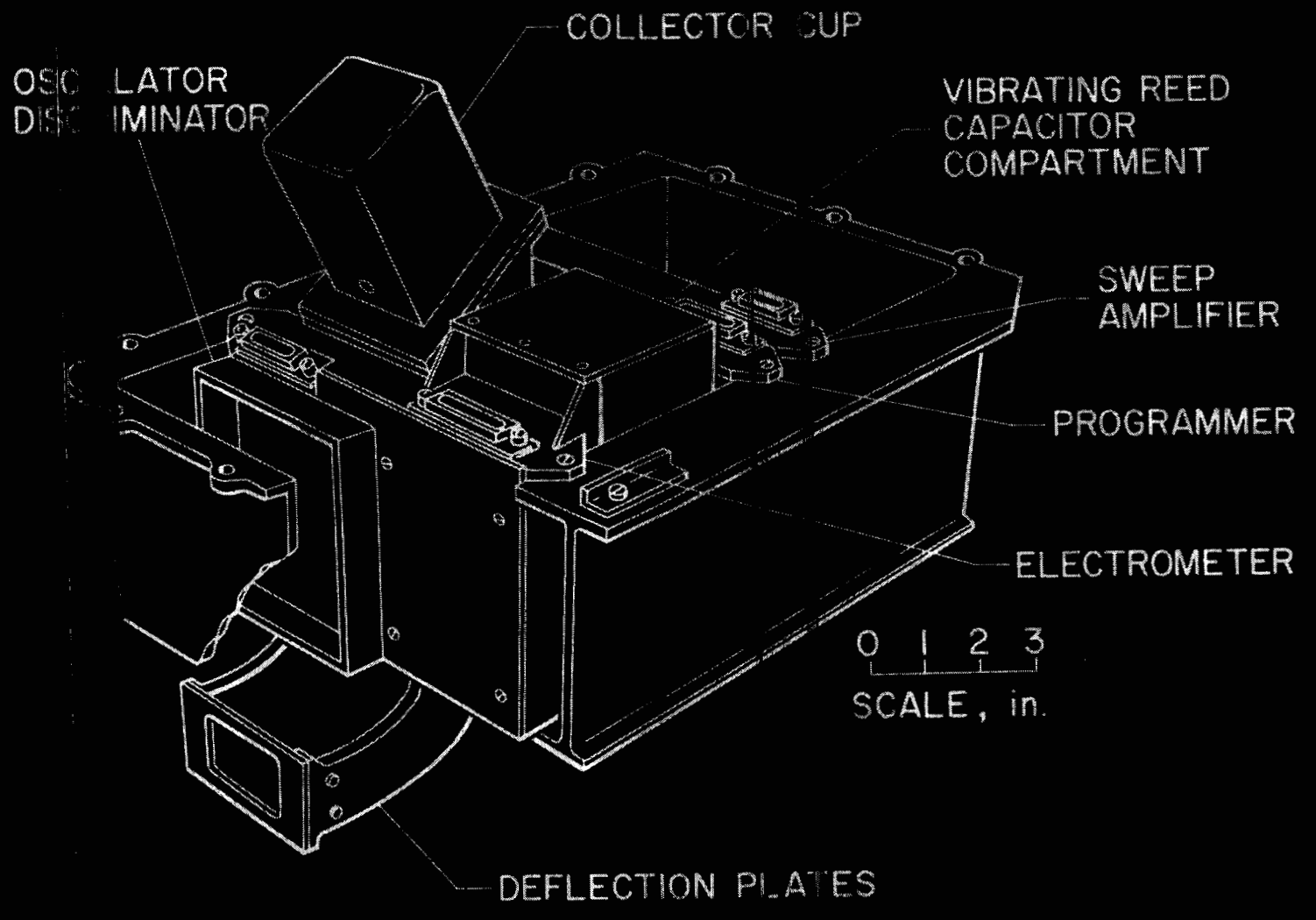
COLLECTOR CUP
OSCILLATOR DISCRIMINATOR
VIBRATING REED CAPACITOR COMPARTMENT
SWEEP AMPLIFIER
PROGRAMMER
ELECTROMETER
0 1 2 3
SCALE, in.
DEFLECTION PLATES

Figure 13.

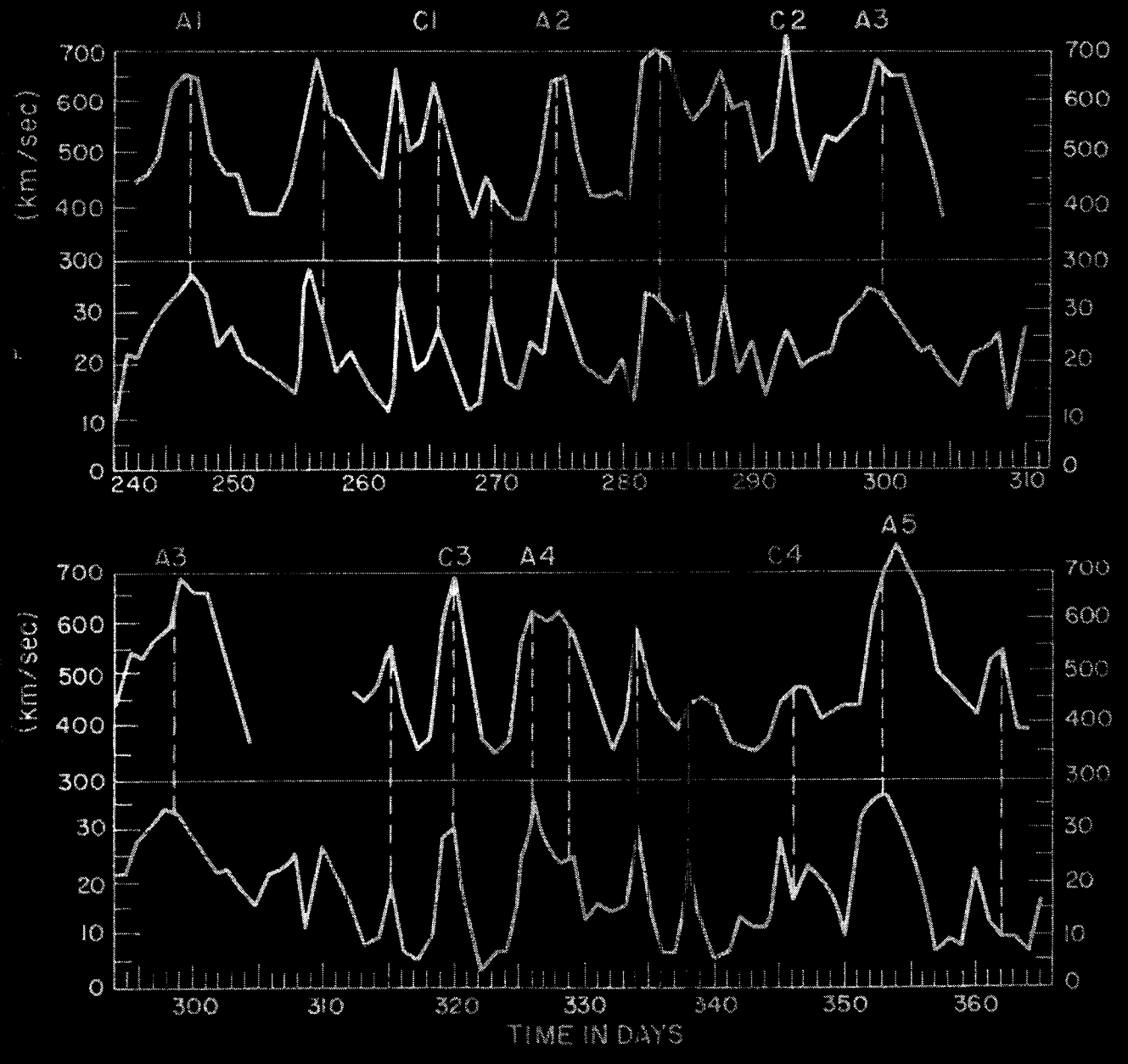
A1
C1
A2
C2
A3
A3
C3
A4
C4
A5
(km/sec)
(km/sec)
700
600
500
400
300
30
20
10
0
240
250
260
270
280
290
300
310
320
330
340
350
360
TIME IN DAYS

Figure 14.

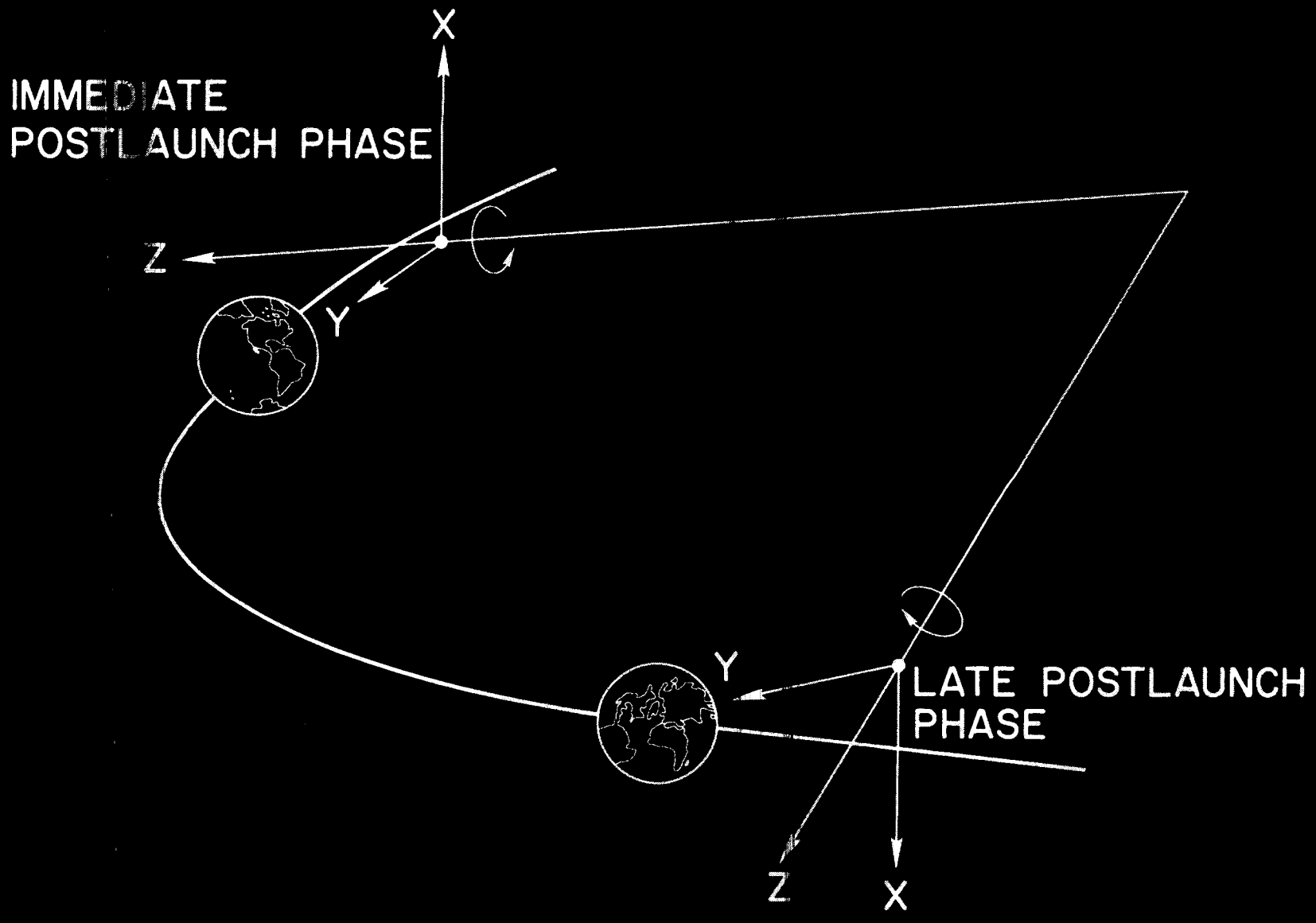

Figure 15.

NATIONAL AERONAUTICS AND SPACE ADMINISTRATION
AMES RESEARCH CENTER MOFFETT FIELD, CALIFORNIA

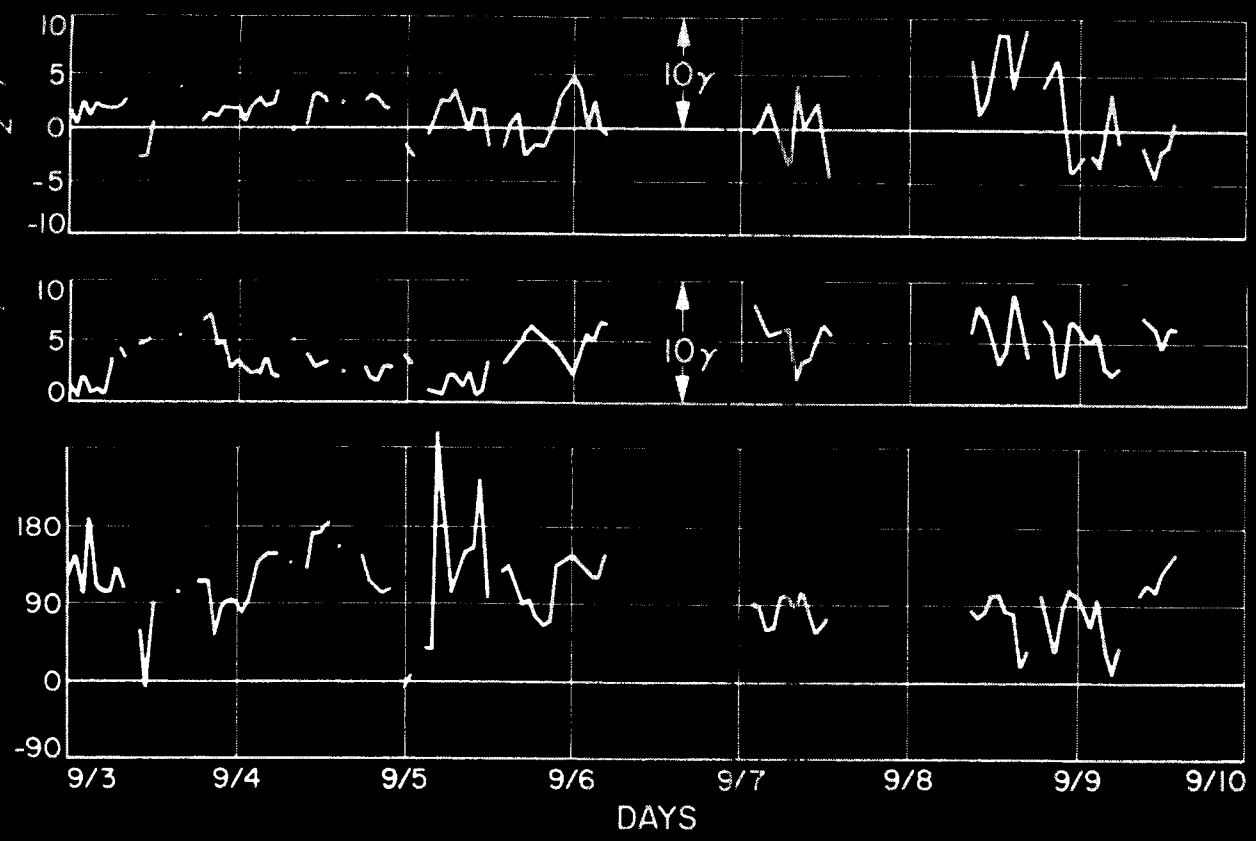

Figure 16.

NATIONAL AERONAUTICS AND SPACE ADMINISTRATION
AMES RESEARCH CENTER MOFFETT FIELD, CALIFORNIA

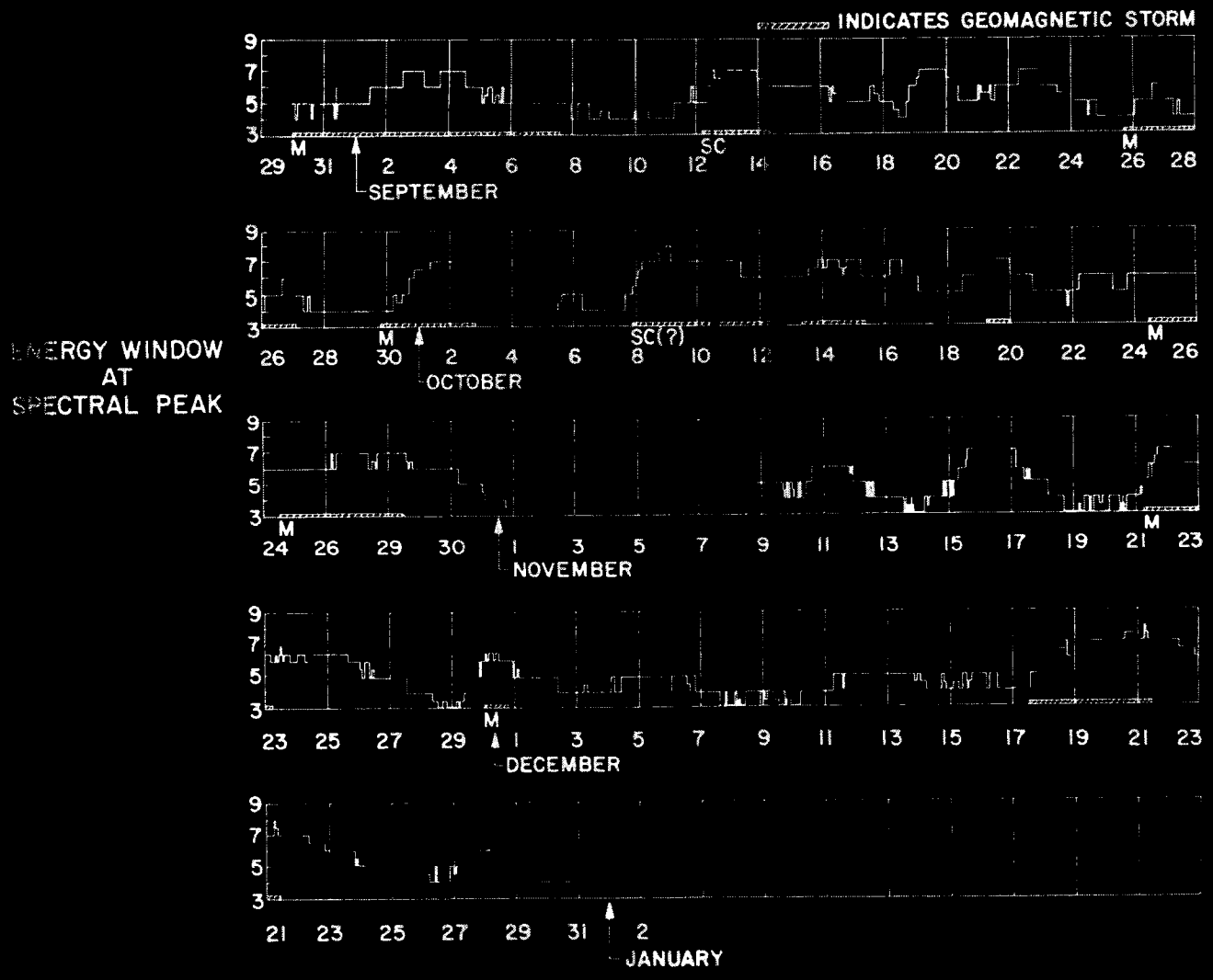

Figure 17.

NATIONAL AERONAUTICS AND SPACE ADMINISTRATION
AMES RESEARCH CENTER, MOFFETT FIELD, CALIFORNIA

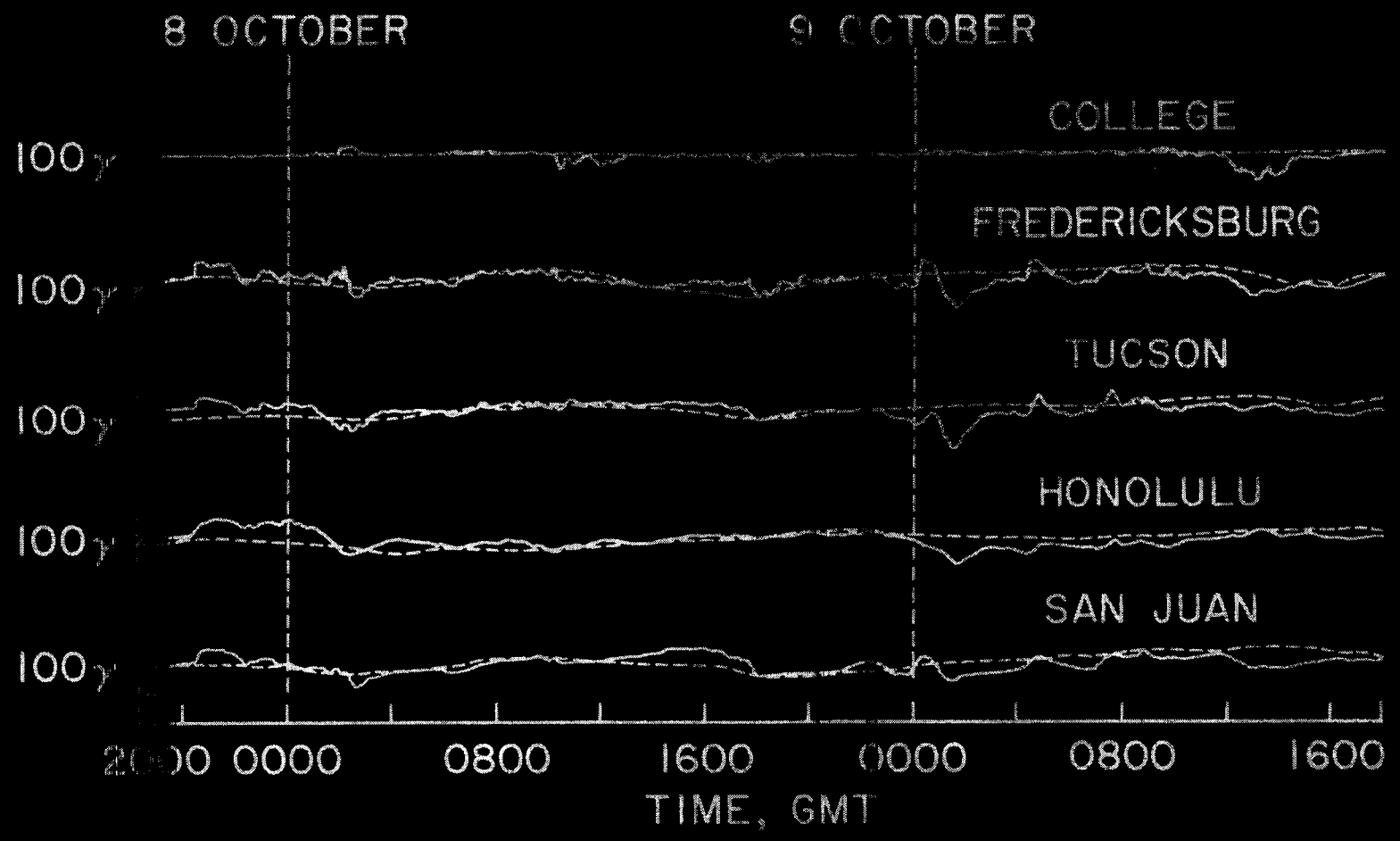
8 OCTOBER
9 OCTOBER
COLLEGE
100γ
FREDERICKSBURG
100γ
TUCSON
100γ
HONOLULU
100γ
SAN JUAN
100γ
2000 0000
0800
1600
0000
0800
1600
TIME, GMT

Figure 2.

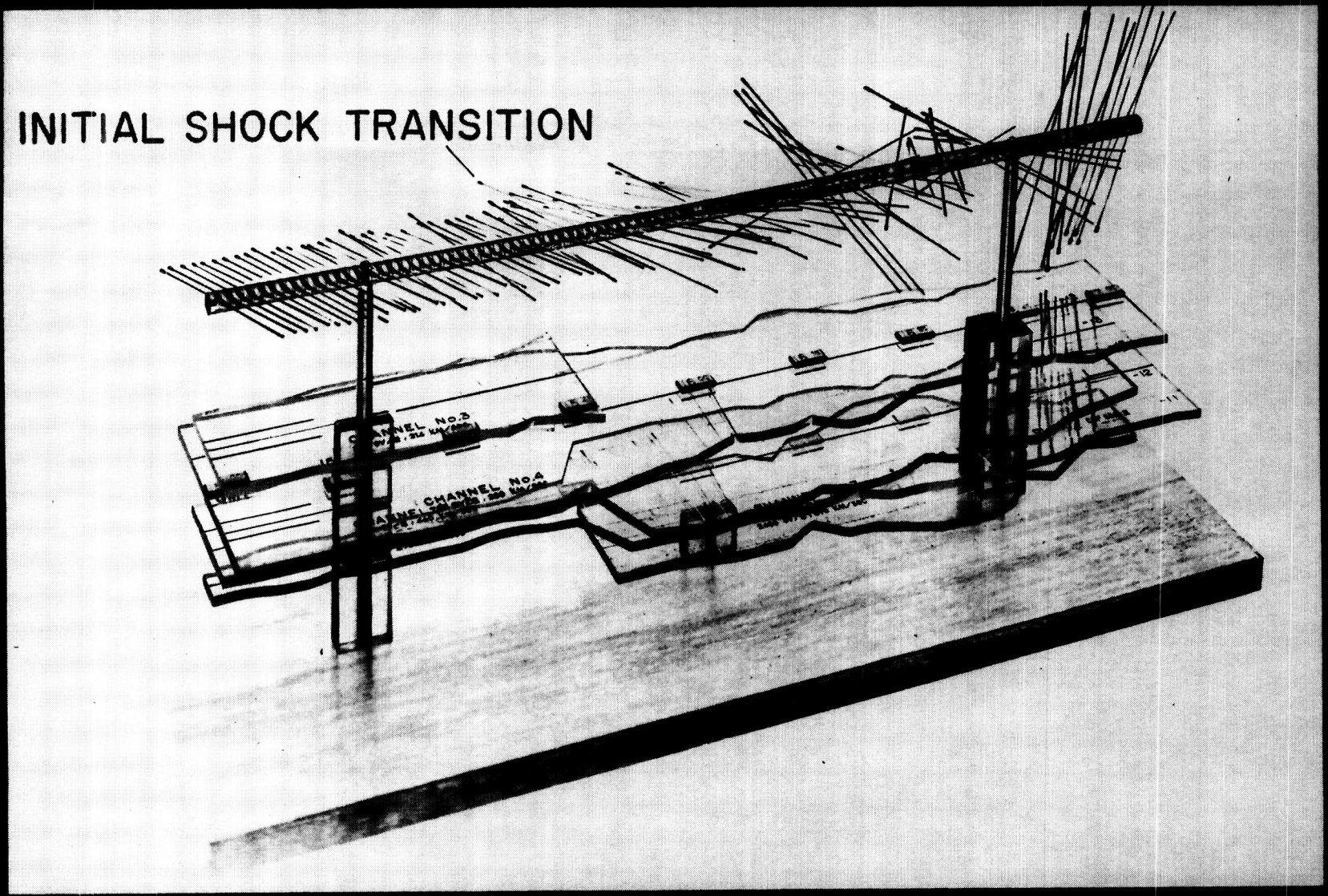

Figure 19.

NATIONAL AERONAUTICS AND SPACE ADMINISTRATION
AMES RESEARCH CENTER, MOFFETT FIELD, CALIFORNIA

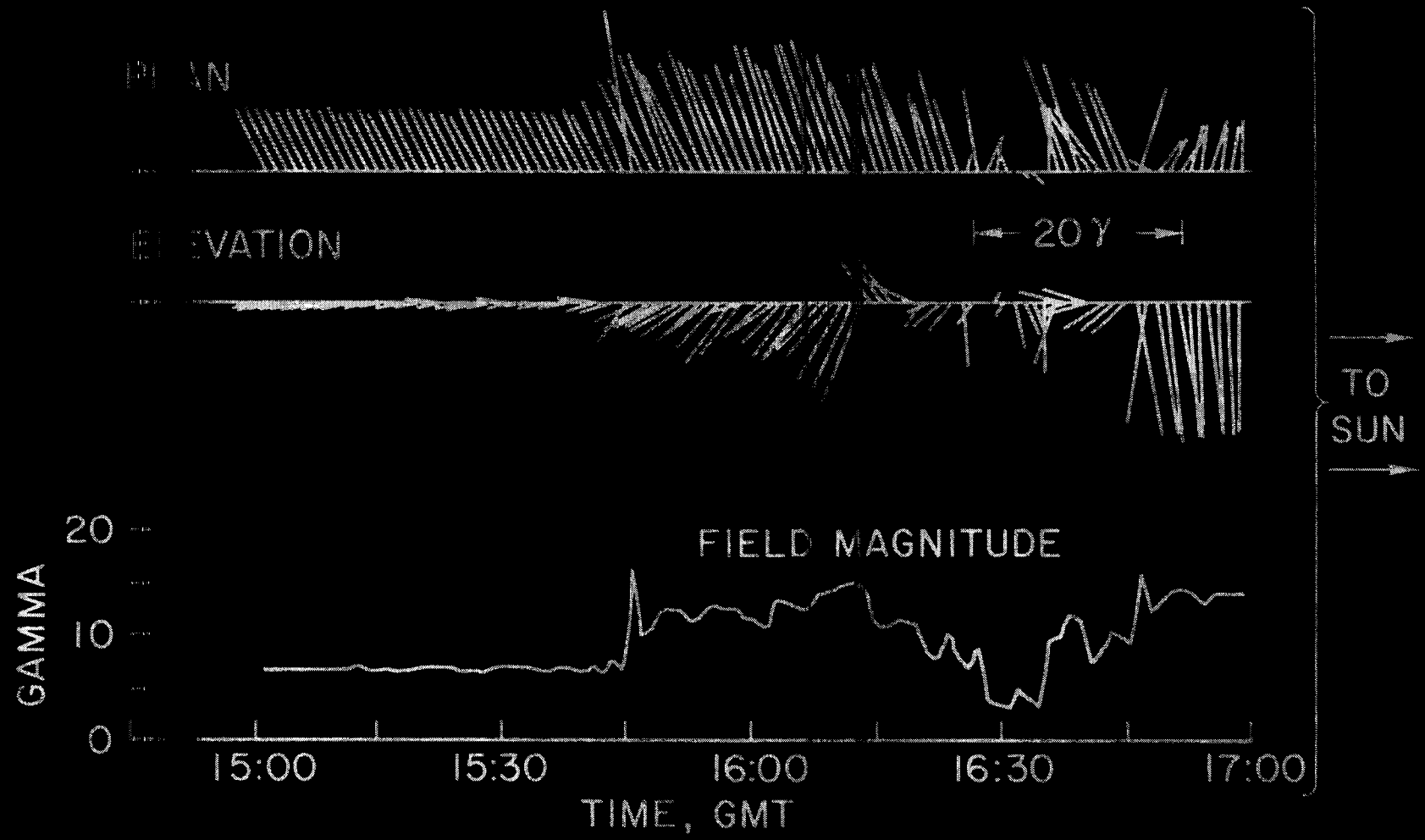
AZIMUTH
ELEVATION
20 γ
TO SUN
FIELD MAGNITUDE
GAMMA
20
10
0
15:00
15:30
16:00
16:30
17:00
TIME, GMT

Figure 20.

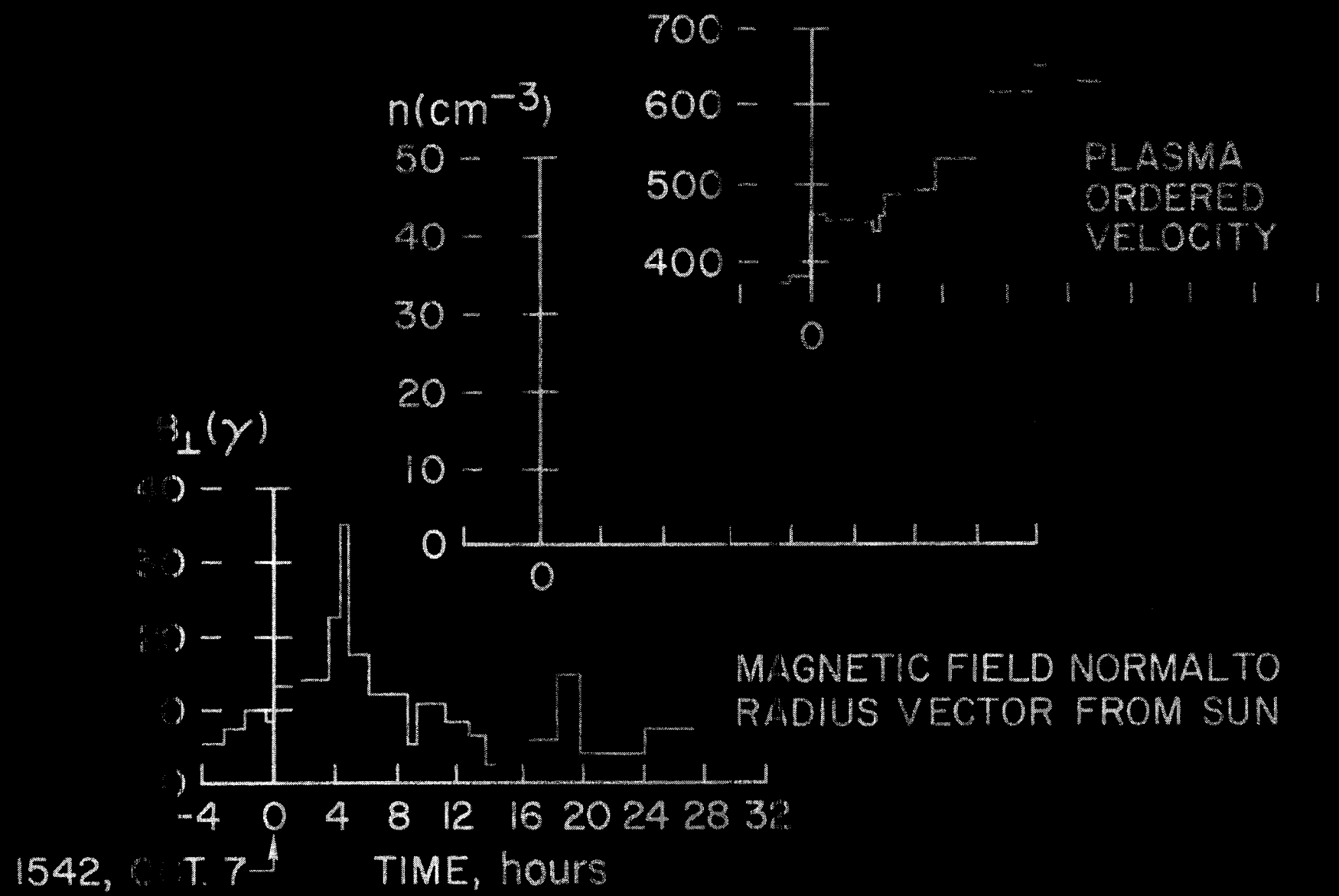
700
600
500
400
PLASMA
ORDERED
VELOCITY
0
n(cm⁻³)
50
40
30
20
10
0
0
B⊥(γ)
-4
0
4
8
12
16
20
24
28
MAGNETIC FIELD NORMAL TO
RADIUS VECTOR FROM SUN
1542, OCT. 7
TIME, hours

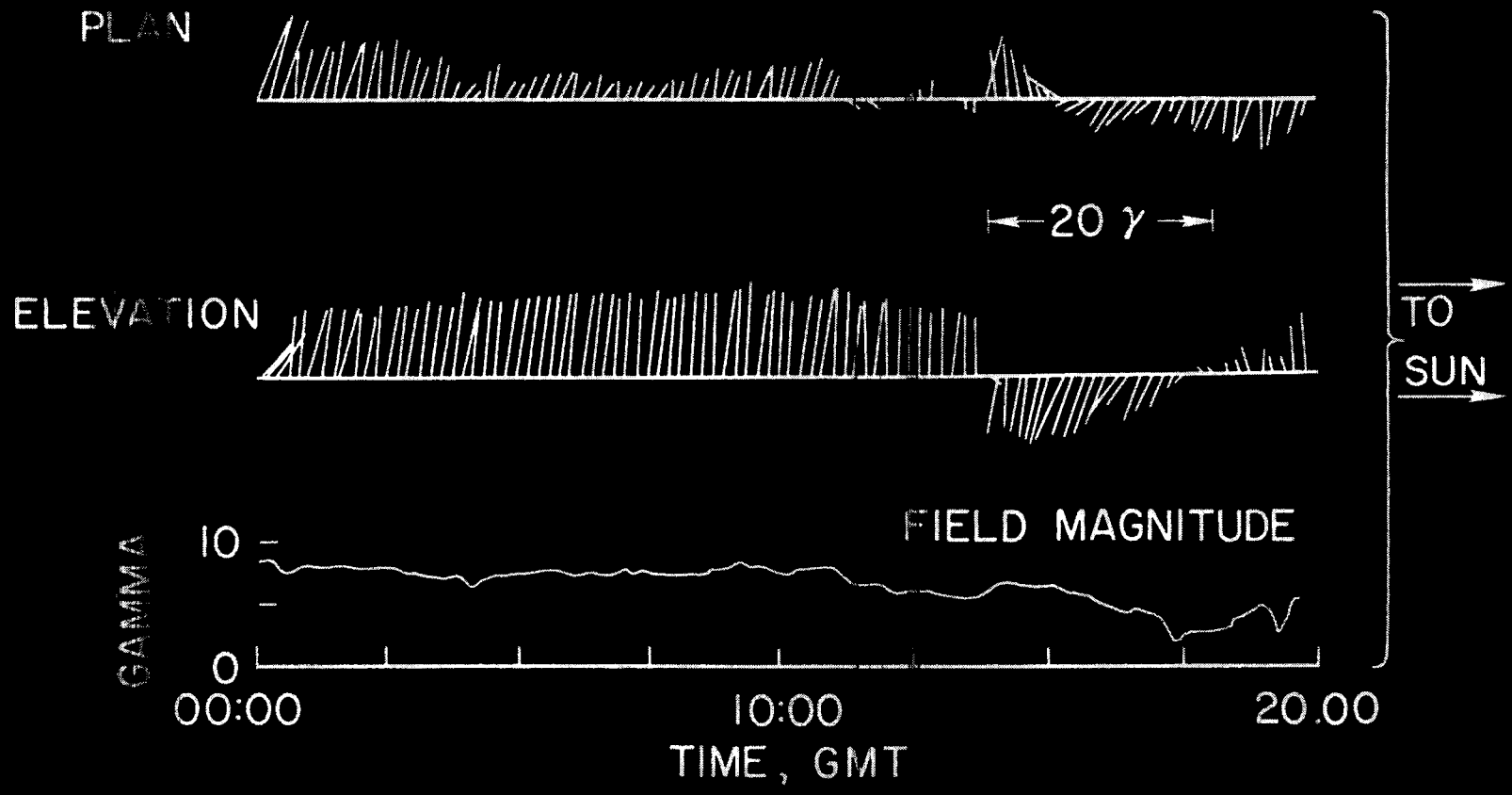

Figure 22.

NATIONAL AERONAUTICS AND SPACE ADMINISTRATION
AMES RESEARCH CENTER, MOFFETT FIELD, CALIFORNIA